

Software Tool for Brain Morphometry Analysis

by

Liew Qiao Jun

18478

Dissertation submitted in partial fulfilment of

the requirements for the

Bachelor of Engineering (Hons)

(Electrical and Electronics)

JANUARY 2017

Universiti Teknologi PETRONAS

Bandar Seri Iskandar

31750 Tronoh

Perak Darul Ridzuan

TABLE OF CONTENTS

CERTIFICATION OF APPROVAL	V
CERTIFICATION OF ORIGINALITY	VI
ABSTRACT	VII
ACKNOWLEDGEMENT	VIII
CHAPTER 1 INTRODUCTION	1
1.1 Background.....	1
1.2 Problem Statement.....	2
1.3 Objectives	3
1.4 Scope of the Project.....	3
CHAPTER 2 LITERATURE REVIEW	4
2.1 Human Brain.....	4
2.2 Magnetic Resonance Imaging (MRI)	8
2.3 Brain Morphometry	10
2.4 Principal Component Analysis (PCA).....	15
2.5 Principal Geodesic Analysis (PGA)	18
2.6 FreeSurfer	20
2.7 Spharm-pdm	23
CHAPTER 3 METHODOLOGY	25
3.1 Research Methodology	25
3.2 Project Activity.....	26
3.3 Gantt Chart and Milestone of FYP	27
3.4 Data Acquisition	28
3.5 Data Pre-processing.....	29
3.6 Subcortical Segmentation	31
3.7 Principal Component Analysis (PCA).....	32
3.8 Spharm-pdm	33
CHAPTER 4 RESULTS AND DISCUSSION	35
4.1 Data Pre-processing.....	35
4.2 Subcortical Segmentation	36
4.3 Principal Component Analysis (PCA).....	38

4.4 3d Image Visualization.....	39
4.5 Voxel Volume.....	41
4.6 Boundary Shape Analysis via SPHARM	43
4.7 Medial Shape Analysis	45
CHAPTER 6 CONCLUSION AND FUTURE WORK	46
REFERENCES.....	47
APPENDICES	53
Appendix A : Subcortical Segmentation	53
Appendix B : PCA.....	54
Appendix C : Visualization Tools	55
Appendix D : Voxel Volume.....	57

LIST OF FIGURES

Figure 1: Human nervous system [55].....	4
Figure 2: Surface of cerebrum [56].....	5
Figure 3: Skull structures[56]	6
Figure 4: The cerebrum can be divided into four lobes [56].....	6
Figure 5 : Cortical and Subcortical region[37]	7
Figure 6: Sequence Parameter [57].....	8
Figure 7 : T1-weighted MRI [58].....	9
Figure 8: T2-weighted MRI [58]	9
Figure 9: VBM process [12].....	11
Figure 10: Difference of PCA and PGA [24].....	18
Figure 11: Intrinsic Mean Algorithm	18
Figure 12: Principal Geodesic Analysis Algorithm	19
Figure 13 : nu.mgz [26]	21
Figure 14 : orig.mgz [26]	21
Figure 15: Before and After Skull Strip [26]	22
Figure 16 : Automatic Segmentation File (aseg.mgz) [26]	22
Figure 17 : Spharm-pdm Workflow [53]	23
Figure 18 : Spharm-pdm shape analysis pipeline [53].....	24
Figure 19: Project Activity Flow	26
Figure 20: Gantt Chart for FYP.....	27
Figure 21: T1-weighted MRI (axial plane).....	28
Figure 22 : T1-weighted MRI (sagittal plane)	28
Figure 23 : T1-weighted MRI (coronal plane).....	28
Figure 24 : Data Pre-processing Flow	29
Figure 25 : After Skull Strip.....	30
Figure 26 : Before Skull Strip.....	30
Figure 27 : PCA Flow	32
Figure 28 : Spharm-pdm parameter	33
Figure 29: Spharm-pdm flowchart	34
Figure 30: Snapshot of aseg file that show the label 41	35
Figure 31: Hippocampus Segmentation (front view)	36
Figure 32: Hippocampus Segmentation (side view).....	37
Figure 33: Hippocampus Segmentation (top view).....	37

Figure 34: Hippocampus Segmentation (3d view).....	37
Figure 35:First Three PCA direction of hippocampus.....	38
Figure 36:3d visualization tool.....	39
Figure 37: 3d visualization of two hippocampus with rotation	40
Figure 38:3d visualization with two hippocampus overlay.....	40
Figure 39: Voxel count for normal group subject 001.....	41
Figure 40: Voxel Count for normal group subject 001 (ITK-Snap)	41
Figure 41 : Voxel volume of hippocampus for each subject	42
Figure 42 : Boundary Shape Analysis of sub002 and sub003(Top: Left hippocampus) (Bottom: Right hippocampus).....	43
Figure 43 : Medial shape analysis of sub004	45

LIST OF FIGURES

Table 1: Volumetric Processing Stages.....	20
--	----

CERTIFICATION OF APPROVAL

Software Tool for Brain Morphometry Analysis

By

Liew Qiao Jun

18478

A project dissertation submitted to the
Department of Electrical & Electronics Engineering
Universiti Teknologi PETRONAS
in partial fulfilment of the requirement for the
Bachelor of Engineering (Hons)
(Electrical & Electronics Engineering)

Approved by,

Dr HO TATT WEI

UNIVERSITI TEKNOLOGI PETRONAS

TRONOH, PERAK

January 2017

CERTIFICATION OF ORIGINALITY

This is to certify that I am responsible for the work submitted in this project, that the original work is my own except as specified in the references and acknowledgements, and that the original work contained herein have not been undertaken or done by unspecified sources or persons.

LIEW QIAO JUN

ABSTRACT

Brain morphometry is a technique to study and analyse parameters such as the volume, orientation, position, cross-sectional area, and thickness of the sub-cortical brain regions. It is used to investigate the signature changes of brain regions or the brain abnormalities and is a potential biomarker of diseases in clinical practice. Although there are open source tools exist to perform the brain morphometry analysis, clinicians do not have access of it due to the tools are hard to use and some of the tools do not provide the normal group database for comparison. Clinicians require a visualization and workflow tool in an easy to use format to allow them to investigate shape changes in the subcortical region. In this thesis, we studied 20 healthy control subjects (10 females and 10 males, range of age:19-55). Their T1-weighted MRI data are pre-processed via the FreeSurfer to get the automated segmentation file (aseg.mgz). The hippocampus (left hippocampus:17, right hippocampus:53) is extracted out for further processing. The medial shape analysis and boundary shape analysis are used to analyse the shape changes of the region of interest. The visualisation tool is created to visualise and compare between two subject. The visualisation tool allow users to rotate, move and overlay two subject in order to find out the shape differences between two subjects.

ACKNOWLEDGEMENT

Foremost, I would like to grip this opportunity to express my greatest appreciation to every people who guide, motivate and help me in completing my Final Year Project (FYP). With their assistance and encouragement, I am able to complete my FYP successfully.

I want to express my sincere thanks to my supervisor, Dr Ho Tatt Wei. He has given me the tremendous support and acknowledgement throughout this period. He has also spent his time to share his expertise and knowledge in this field of study.

I would like to show my gratitude to CASILab at The University of North Carolina at Chapel Hill distributed by the MIDAS Data Server at Kitware, Inc for providing me the T1-weighted MRI data of healthy subjects used in this paper.

Not to forget, I am indebted to everyone who helping me whenever I felt difficulties. Last but not least, I also want to thank my dear family for their understanding and supports on me during this period.

CHAPTER 1 INTRODUCTION

1.1 Background

In the last decade, shape analysis is a widely research topic with findings in several fields such as agriculture, biology, and neuroscience. Brain morphometry is one type of shape analysis that gets the hot interest in neuroscience recently since the magnetic resonance imaging (MRI) technique is widely used in the clinical practice. The ability of MRI is impressive for displaying the cross-sectional of brain and allow the clinician to visualize epileptogenic brain lesions by using some techniques such as 3d reformatting to enhanced the MRI image. The brain morphometry has been hypothesized to have connection to various neurogenerative brain disorder [28][29]. In order to prove this, many research studies that are related to brain morphometry are carried out. According to [1] and [2], a study of Temporal Lobe Epilepsy (TLE) is done by analysing the shape of subcortical structures. The pathological findings in [1] and [2], the shape of the hippocampus is observed to be atrophied in patients with TLE. Since there exist many studies that have already proven the atrophy of hippocampus region are related to TLE, this project is to create a software tool to observe, compare and analyse the shape changes of hippocampus across different subject groups.

In this project, the T1-weighted MRI data was processed using the FreeSurfer tool, the shape and volume changes across various brain structures are examined and analysed. In this stage, the project is performed on hippocampus, but it is useful for other subcortical regions of the brain. This project is also to further facilitate the investigation and relate between structural brain phenotype and disease stage progression. It is hoped that such tools will permit researchers and medical practitioners to identify brain regions affected by disease and perhaps even work out any causal or sequence of degradation and potential target areas for brain therapy.

1.2 Problem Statement

Brain morphometry analysis has the potential to precisely locate the brain morphological changes between the healthy and pathological structures. Although open source tools exist to compute these measurements, clinicians do not have access to these tools in an easy to use format and neither does there exist a reference database of normal patients to compare against. Since subcortical brain volume is affected, a further question to be investigated is if specific morphological changes can be identified for region of interest- this include shape specific atrophy and rotations. There is a need to develop analytics, visualization, and workflow tools for clinicians to enable investigation of the effect / correlation of the brain region morphology.

1.3 Objectives

The objectives of this projects are: -

- To develop visualization and workflow tool for clinicians to compare brain region volume and position
- To incorporate population level reference images into the comparison tool in (1) and to develop simple statistically analysis
- To develop advanced analysis of morphological parameters of sub-cortical brain regions

1.4 Scope of the Project

Scope of study defines the limits or boundary for the particular project study. Hence, it is very important for the scope to be within study and not out of topic. In this project, several topics have been focused: -

- Automated software shape analysis to describe the shape and orientation of the sub cortical brain regions, which mainly focus on hippocampus segment
- To compare the volume and shape between normal control group and patients

CHAPTER 2 LITERATURE REVIEW

2.1 Human Brain

The human brain is an amazing and important organ that located at the head and protected by the skull. The weight of adult human brain is around 1.2 to 1.4kg which occupied approximately 2% of the body[30]. According to [31], the average brain volume of men (around $1260mm^3$) is bigger than women (around $1130mm^3$). The function of the brain is to controls all function in the body such as emotion, motion, intelligence, memory, creativity, thought and speech. Generally, the brain receives the information through five sense (smell, hearing, taste, sight and touch), interpret and analysis it, store the information in memory and the decisions are send to the body to act accordingly whenever it is necessary.

Undeniable, the human brain plays an important role in the nervous system. The nervous system can be divided into two major parts which are central nervous system(CNS) and peripheral nervous system(PNS). The CNS consists of human brain and spinal cord. It is responsible for the analysis of information, body coordination and decision making for human body activities. The PNS consists of nerves that branch out from the spinal cord and from the human brain [32] and responsible for the automatic nervous system activities such as heart rate, breathing rate, sweating, secretion of hormones and digestion.

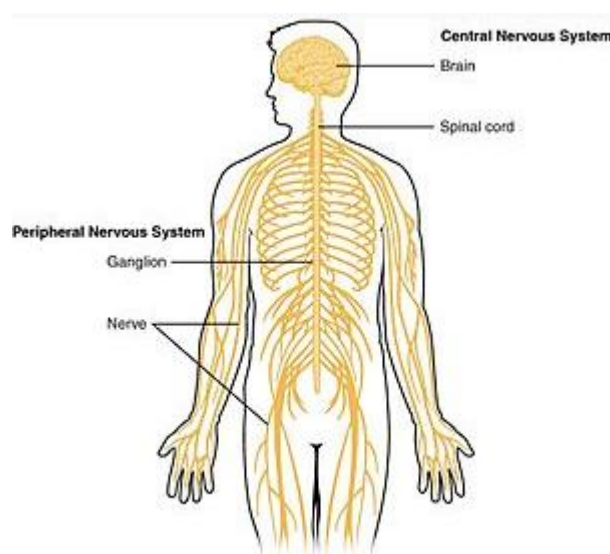


Figure 1: Human nervous system [55]

There are many ways of dividing the brain anatomically into regions. One of the common way is to divide the brain into three parts which are cerebellum, cerebrum and brainstem[3-5].

a) Cerebrum

Largest part of the human brain is cerebrum and it can be divided into left and right cerebral hemispheres which are covered by the cortex. It is mainly responsible for memory, speech, learning, emotional responses and five senses. The surface of the cerebrum is known as cortex which is made up of grey matter and in folded appearance to increase the surface area to allow more neurons fitted inside the skull [33]. The fold for the cortex is known as gyrus while the groove between the fold is known as sulcus. The white matter is located under the cortex and made up by the axons which connect between neurons, and send information across different parts of brain areas.



Figure 2: Surface of cerebrum [56]

The cerebrum is divided into left and right cerebral hemispheres. The left and right hemispheres are connected through by the bundle of fibres which is known as the corpus callosum for sending the signal from one to another hemisphere. Each of the hemisphere controls another side of the body. Besides that, each of the cerebral hemisphere can be categorised into four lobes which are frontal lobe, temporal lobe, parietal lobe and occipital lobe. According to [34], the name of the lobes is based on the name of the skull bones that overlie them. Each of the lobe is responsible for one or two specific functions. However, the lobe does not operate alone. They work with other lobes to provide a more complex system for human activities [35].

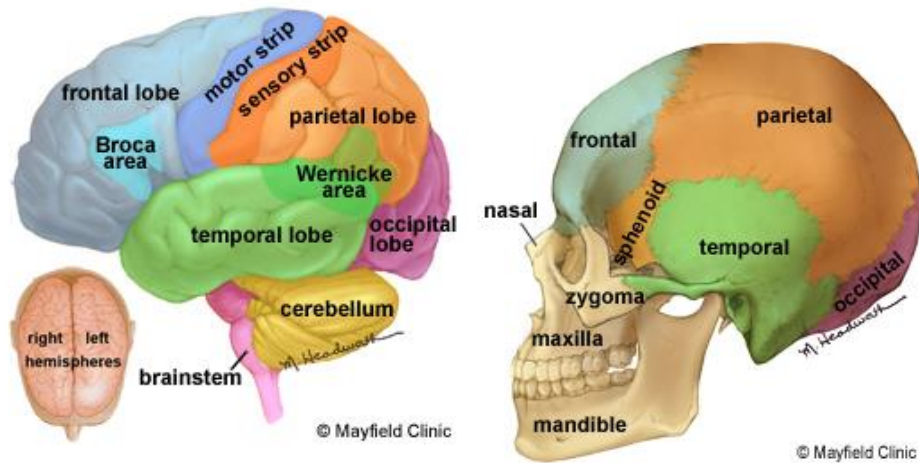


Figure 4: The cerebrum can be divided into four lobes [56]

Figure 3: Skull structures[56]

b) Cerebellum

The cerebellum is located below the cerebrum and it consists of a thinner outer cortex. Same to the cerebrum, the outer part of cortex is grey matter while the inner part of the cortex consists of the white matter and its surface is richly folded. The cerebellum is connected to the brainstem by the superior cerebellar peduncles [36]. The cerebellum is mainly to control the balance of human body and to coordinate muscle movements.

c) Brainstem

The brainstem is made up by midbrain, pons and medulla which are located at the back part of the skull. It connects the brain and the spinal cord [36]. It is mainly responsible for the involuntary function such as respiration, sweating, blood pressure, heart rate, vomiting, digestion and many other.

To many research studies, they classified the human brain into cortical and subcortical regions. The cortical region is the surface of the brain which is known as cerebral cortex. While the subcortical regions are the regions that locate below the cerebral cortex which includes the brain stem, hypothalamus, limbic system, cerebellum, thalamus and so on [37].

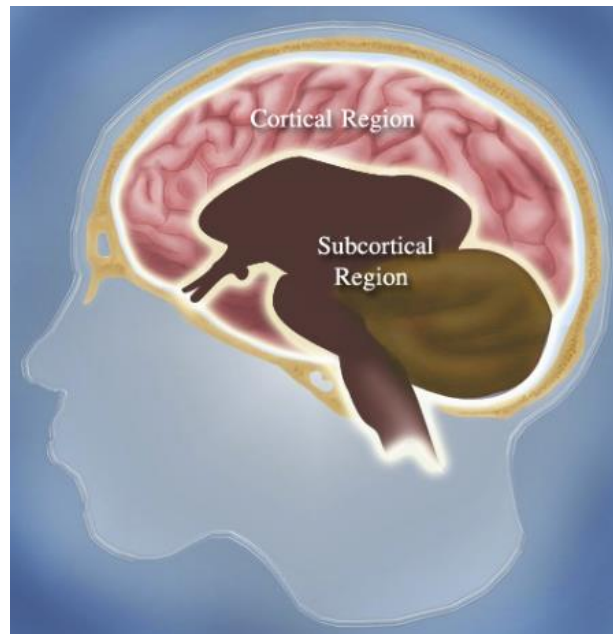


Figure 5 : Cortical and Subcortical region[37]

Although human brain is protected by skull, it can encounter damage. For example, the neurodegenerative diseases cause damage. When some part of the regions in brain are damaged, it causes abnormalities in functionality such as brain tumour or cancer can affect lost of functions in hearing, sighting and motion. The Alzheimer's disease is evident for causing damage in hippocampus. According to the research, nerve cell in the hippocampus is the first part in the brain that is damaged by the Alzheimer's disease [6]. Hippocampus belongs to limbic system and it can be divided into left and right. Its plays important role in memory and navigation. The failure of hippocampus results the memory loss, disorientation and unable to remember the new thing such as location which are the symptoms of the Alzheimer's diseases [7].

2.2 Magnetic Resonance Imaging (MRI)

Magnetic Resonance Imaging (MRI) is a medical imaging technique that is commonly used in radiology to generate the pictures of the body using a powerful magnetic scanner. The MRI scanners use radio waves and magnetic field to create detailed images of the region of interest across the body [43]. Unlike the computed tomography scan (CT scan), MRI does not use x-rays. Although the hazard of x-rays is known for its well-controlled in medical contexts, MRI is considered slightly better than CT scan in term of its ability to differentiate different kinds of tissues. However, MRI takes longer time to acquire images compared to the CT scan.

During MRI scan, people require removing their metal object because of the metallic subject can affect the accuracy of MRI and cause blurry image. For acquiring the MRI images, people lie inside a tunnel-shaped scanner which contains a strong magnetic [44]. The MRI takes approximately 30 to 60 minutes to scan the regions of interest for particular study. Typically, MRI creates hundreds of images and each of the image is known as slice. It can be stored in the computer and reconstructed for the model in three dimension [45].

MRI displays the image contrasts that depends on T1, T2 and proton density. In MRI images, the bright colour is the area with high signal while the area with the low signal is shown in dark colour. The grey colour show the area with intermediate signal. By varying the sequence parameter such as Repetition Time(TR) and Time to Echo(TE), different types of the MRI images are created. TR is an amount of time between the RF pulse that applied to the same slice while the TE is the time between RF pulse and echo received [57].

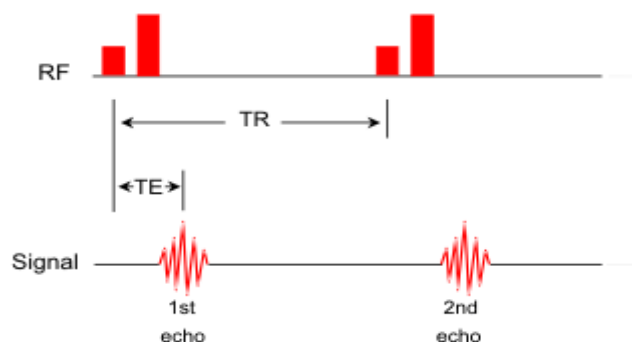


Figure 6: Sequence Parameter [57]

T1-weighted MRI and T2-weighted MRI are the MRI scans that are most commonly used. The T1-weighted MRI is good for display the contrast between the white matter and grey matter. The tissues that contain high fat (white matter) appear bright while the tissue that filled with water (CSF) appear dark. The grey matter is shown in grey colour. The T1-weighted MRI can be produced by using short TE and short TR [46].

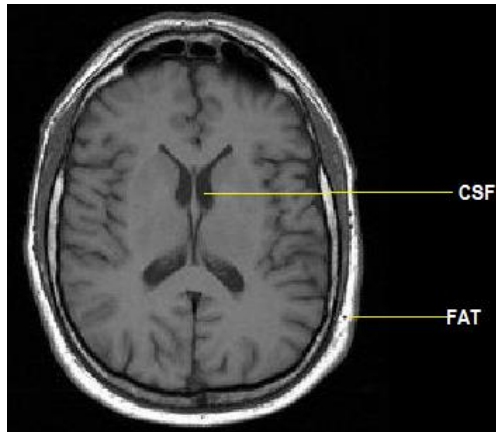


Figure 7 : T1-weighted MRI [58]

The T2-weighted MRI is useful for displaying the contrast between brain tissues and CSF. The tissues that contain high fat (white matter) appears in dark while the tissue that filled with water (CSF) appears in bright. The T2-weighted MRI can be obtained by set the sequence parameter (long TR and long TE) to minimize the T1 relaxation effects [46].

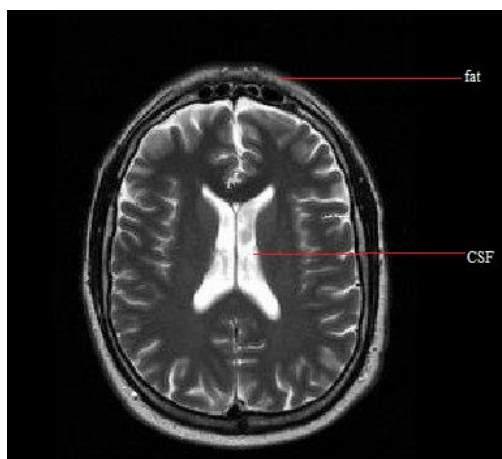


Figure 8: T2-weighted MRI [58]

2.3 Brain Morphometry

Brain morphometry is the combination of the brain sciences and morphometry, which focus on the measurement of the brain structures and analysis of the change of brain in different points of aspect such as sex and age [8]. In short, brain morphometry is used to analyse the physical shape and form of the brain. In order to do the brain morphometry analysis, the magnetic resonance image (MRI) is required as the input. Magnetic resonance image is the image of the brain that is generated using magnetic field and radio waves and it allows clinicians to analyse brain structures based on different aspects such as volume, surface, and shape [9,10]. Brain morphometry can be carried out based on few approaches, which are: -

a. Voxel-based morphometry (VBM)

There are a lot of way to do morphometry analysis and one of the useful way is to analyse the structural difference by comparing the local composition of different brain tissues types such as grey matter. Voxel-based morphometry (VBM) is based on this way by comparing the local concentration of grey matter between two subjects. VBM can be performed by spatially normalizing the MRI images into standard place, then the grey matter is segmented and extracted from the normalized MRI image. Statistical analysis can then be done after grey matter image has been smoothed by convolving with an isotropic Gaussian Kernel. The regions of grey matter that changes significantly among the groups are shown in Statistical Parametric Map (SPM) which knowns as the output of the VBM. [11-12]

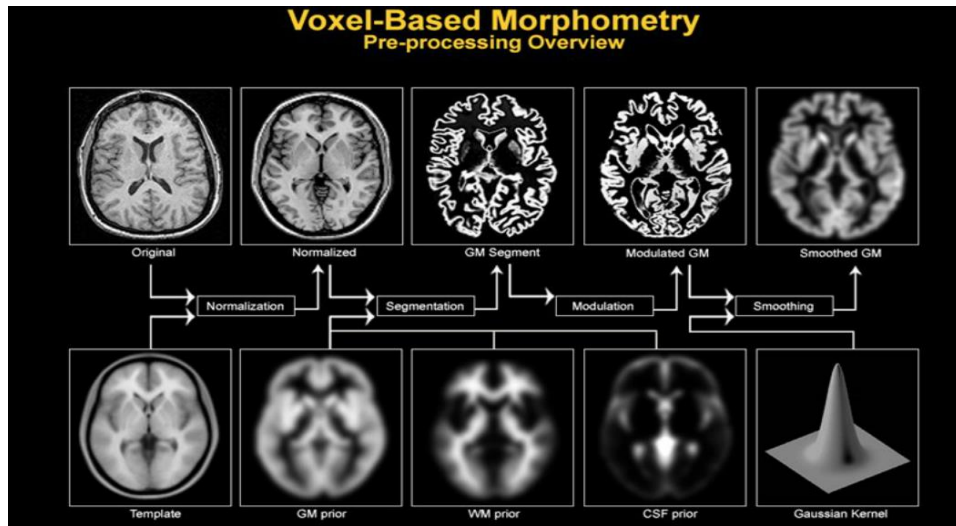


Figure 9: VBM process [12]

Each of the images is required to be registered into the same template image in order to align the images across each other into the stereotactic space. Next, normalization is performed in two steps, which are linear transformation and nonlinear transformation. In linear transformation, each of the image needs to be matched into the same template using the 12-parameter affine transformation which fits the overall shape and size by minimizing the square distance of parameters with expected values and mean-squared difference between the template image and source image [12].

For the nonlinear transformation, a linear combination of low frequency periodic basis functions is modelled for the global nonlinear shape differences [13]. In order to minimize the squared difference between MRI image and template image, the coefficients of the basic functions are needed to be estimated and the smoothness of the deformations is enhanced at the same time. The registration quality is important so that the final solution is not biased by the template image that is chosen. Hence, the average of a great number of MR images are in the similar stereotactic space which is an ideal template for many research studies. The resolution of the spatially normalised images have to be in high resolution which is 1 or 1.5 mm isotropic voxel so that partial volume effects is not influenced by the segmentation of grey matter.

After spatial normalization, the image is then partitioned or segmented into different brain tissues types such as grey matter(GM), white matter(WM) etc. The issues of non-uniformity image intensity are corrected in this segmentation step which is the result of position of cranial structures within the different MRI coils [14]. The grey matter image is then smoothed by convolving with an isotropic Gaussian Kernel. The size of the kernel is important and should get approximated to the size of expected regional differences among the groups of subjects. One of the reasons for smoothing is to make every voxel having the average concentration of grey matter. Besides that, parametric statistical test's validity is enhanced by the smoothing step because of the data rendering is distributed normally by central limit theorem. [12].

The last step of the VBM is performed the statistical analysis using the general linear model (GLM). There are many tests, group comparison and grey matter concentration identification are done in the GLM. The SPM consists all the result of statistical tests that been done in GLM. Some of the corrections need to be done for the multiple dependent comparisons [13].

One of the advantages of VBM is that it does not require priori assumption about ROIs due to VBM is a whole brain analysis and has been fully automated. VBM is not biased to anyone of the structures by giving comprehensive assessment of anatomical differences throughout the brain [13]. Moreover, the VBM technique can either be used with diseases subject or heathy subject. For example, studies on structural brain differences utilizing this method have already been carried out based on a variety of diseases such as Down's syndrome, Parkinson's syndrome, Bipolar disorder, temporal lobe epilepsy and etc. in recent years. According to [14], a study of Schizophrenia is done by analysing the deficits in brain volume using VBM. In this experiment, there were 390 patients with Schizophrenia taken as the objects compared with 364 healthy control group. Two finding can be concluded in this study, the most significant finding is the left medial temporal lobe and left superior temporal gyrus deficits in patients with Schizophrenia. Besides that, patients with Schizophrenia lack of grey matter and white matter compared with normal control group. Abnormality of brain regions in schizophrenia can be identified

by using the whole-brain analysis which is VBM and then validated it by using ROI analysis.

According to [19], there is a research completed with this method to know the effect of brain morphometry and the duration of illness on geriatric depression based on VBM method. 30 patients with depression is compared to 47 normal group in this research and found that the right side hippocampus's volume of the patients had smaller size than normal people. Another significant finding was the hippocampal-entorhinal cortex's volume is inversely proportional to the duration of illness. The researches show that some of the diseases such as Alzheimer's and Schizophrenia belongs to distinctions of morphometry in particular region.

b. Deformation-based morphometry (DBM)

Deformation-based morphometry is non-linear registration algorithms that use deformation fields to analyse the position differences within the brains.

The process of spatially normalization registers each of the images to the same template image in order to align the images into stereotactic space. Each of the normalized image will have one deformation field which can be known as 3D vector field (each point consists 3 element vector) and it is resulted by mapping every voxel in the source image to voxel in the template image. Hence, each of the lattice location corresponds to the location in the template image. In other word, voxels that are located in each of the deformation field have the same location in the un-warped images and statistical analysis can be performed by comparing the position of the subject. The canonical variates analysis and Multivariate analysis of covariance can be used produced the results [15].

The advantages of DBM is that it does not require priori assumption about ROIs due to DBM is a whole brain analysis and fully automated which is similar as VBM [16]. Again, DBM is not biased to anyone of the structures by

giving comprehensive assessment of anatomical differences throughout the brain [15].

c. Surface-based morphometry

Surface-based morphology, one of the morphometry analyses, is to reconstruct the surface based on the boundary between different classes of tissue after the segmentation has been performed in the brain. The surface reconstruction can be described as the process by which atoms at the surface presume not same in construction than that of the bulk. It is so important for the morphometry analysis to continue to the gyrification process. It can be used to study the cortical thinking and the major depressive disorder (MDD) which is described as the characteristic mood disturbances with the social functional impairment in patients [17].

d. Diffusion-weighted MR-based brain morphometry

The development of Magnetic Resonance Imaging (MRI) has make the nerve fibre-tracking techniques being the latest offspring of the MR-based morphological approaches. Using this approach, the tract of the nerve fibres can be delineated via the diffusion tensor imaging (DTI) by observing the displacement distribution of the water molecules within each voxel in the entire MRI scan. Since the DTI is powerful to extract and depict the diffusion anisotropy effects on the fibre tracks, and fully illustrate the details on the brain tissue microstructure, the DTI has been widely used in demonstrating the subtle abnormalities in many diseases like schizophrenia and stroke [18].

2.4 Principal Component Analysis (PCA)

Principal Component Analysis(PCA) is a powerful and useful statistical technique that has widely been used in computer sciences and neuroimaging. It is a common technique for the applied linear algebra and non-parametric method in finding the patterns from a high dimension data, extracting the information from it and reduce the high dimensional data set to a lower dimension without much loss of data or information. Perhaps some hidden information that underlie from the complex data set can be found from it [22].

The purpose of PCA is to re-express a high dimensional or confusing data by computing the most meaningful data. It is important and useful for the experimenter to differentiate which dynamics are important, can be ignored or just redundant. PCA combines the basics of linear algebra and statistical such as means, variance, covariance, matrices, eigenvectors, and eigenvalues.

The PCA can be performed using the following steps. First, collect the data set and perform the data pre-processing on it by calculating the mean for each features, types or dimensions and then subtract the mean from each of the features, so this makes each of the features now have exactly zero mean. This can be known as mean normalization.

$$\text{Mean , } \mu^j = \frac{1}{N} \sum_{i=1}^N x_j^{(i)}$$

where x_j are different dimensions or features (e.g. x_1 is height of students, x_2 is weight of students)

$$x_j^{(i)} = x_j^{(i)} - \mu^j$$

The reason of subtracting the mean from the data is to simplify the variance and covariance equation and make sure the values of variance and covariance are not affected by mean. After that, the covariance between 2 dimensions is calculated and form the covariance matrix. From the covariance, the relationship between the two dimension can be made. If the sign of covariance is positive means both dimensions are increasing or decreasing together. In other words, a negative sign means one increases while the other decreases, or vice-versa. If the covariance is zero indicates both dimensions are independent to each other.

$$cov(X, Y) = \frac{1}{N-1} \sum_{i=1}^N x^i y^i$$

The covariance matrix is a square symmetric $m \times m$ matrix and the diagonal terms of it are the variance of each particular dimensions while the covariance between 2 dimensions are show in off-diagonal.

$$C = \begin{bmatrix} cov(x, x) & cov(x, y) \\ cov(y, x) & cov(y, y) \end{bmatrix}$$

Eigenvectors and eigenvalues of the covariance matrix need to be computed once the covariance matrix is obtained. Eigenvector is a non-zero vector that remains its direction when linear transformation is applied on it and its symbol is v , while the eigenvalue is scalar.

$$A \cdot v = \lambda \cdot v$$

$$(A - \lambda \cdot I) \cdot v = 0$$

Where $A = m \times m$ matrix

$V = m \times 1$ non zero vector

$\lambda = \text{scalar}$

The λ in this equation known as eigenvalues which associated with the eigenvector v . It can be concluded that the value of λ is the eigenvalue of A while the vector v that corresponds to the eigenvalues is the eigenvector of A . As you can see the eigenvalue and eigenvector always come in pairs. Eigenvalues can be found by compute the roots of $(A - \lambda \cdot I)$ and each of the eigenvalues will have an eigenvector. It is important to know the characteristic of eigenvectors which the eigenvectors can be found for the square matrix only and not square matrix has eigenvectors. If the size of square matrix is $n \times n$, there are n numbers of eigenvectors and the eigenvectors are perpendicular to each other regardless the dimension.

The number of dimensions can be reduced by ignoring the less significance components which has the small eigenvalues. Although some of the information would be lost, but the significant information is kept. The principal component of the data set is the eigenvector with the most significance eigenvalue. The final data set can be derived by using the following formulae:

$$\text{Final Data} = \text{Row Feature Vector} * \text{Row Zero Mean Data}$$

The feature vector is the matrix that contains a list of eigenvectors that are arranged based on the corresponding eigenvalues in descending order which from the highest to lowest. After that, the feature vector is transposed to make the eigenvectors represented in row. The Row Zero Mean Data in the equation means the data after being subtracted by the mean values.

In summary, PCA is a simple, non-parametric mathematical tool that use to reduce the high dimension confused data set into lower dimension and extract the most significant information from it. In this project, the PCA method is useful for determine the orientation and the position of the sub cortical brain region (hippocampus) by compute the principal component plane of the brain image.

2.5 Principal Geodesic Analysis (PGA)

Principal Geodesic Analysis is a generalization of principal component analysis. Unlike the PCA which applied in linear transformation, PGA is used in a nonlinear transformation. Figure 8 shows the difference between PCA and PGA of the $P(X)$ for dimension reduction. The blue line indicates PCA while the red line indicates PGA. As you can see, the PCA cannot produce the principal component that located within $P(X)$ while the PGA can produce the geodesic components within the $P(X)$ which can be used for dimension reduction and high accuracy in analysis [24].

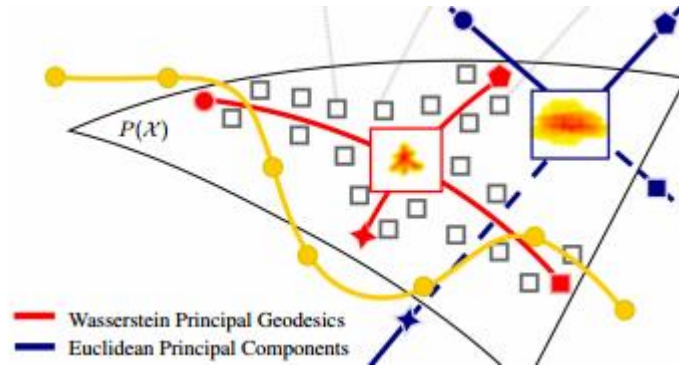


Figure 10: Difference of PCA and PGA [24]

The outcome of PGA is to produce the geodesic components from the manifold valued data which give the maximized variance of data and the minimum loss of information. The geodesic components also can be known as geodesic curve or geodesic sub manifolds. The PGA can be performed by computing the intrinsic mean of the manifold dataset $\{x_1, x_2, \dots, x_n\}$ and finds the geodesic components [26]. The intrinsic mean of manifold dataset is defined as minimizer in the manifold of sum-of-square Riemannian distance to each of the point in dataset [25].

Algorithm 1: Intrinsic Mean

Input: $x_1, \dots, x_N \in M$

Output: $\mu \in M$, the intrinsic mean

$\mu_0 = x_1$

Do

$$\Delta\mu = \frac{\tau}{N} \sum_{i=1}^N \text{Log}_{\mu_j} x_i$$

$$\mu_{j+1} = \text{Exp}_{\mu_j}(\Delta\mu)$$

While $\|\Delta\mu\| > \epsilon$.

Figure 11: Intrinsic Mean Algorithm

The algorithm above shows the method in computing the intrinsic means which will be used later in performing the PGA. The tangent space of manifold at the intrinsic mean are represented by $T_\mu M$. By producing an orthonormal basis of tangent vector $v_1, v_2, \dots \in T_\mu M$ that span the tangent space, the result is known as the geodesic components. The algorithm for principal geodesic analysis on manifold can be computed by [25].

Algorithm 2: Principal Geodesic Analysis

Input: $x_1, \dots, x_N \in M$

Output: Principal directions, $v_k \in T_\mu M$

Variiances, $\lambda_k \in \mathbb{R}$

$\mu =$ intrinsic mean of $\{x_i\}$ (Algorithm 1)

$u_i = \text{Log}_\mu(x_i)$

$S = \frac{1}{N} \sum_{i=1}^N u_i u_i^T$

$\{v_k, \lambda_k\} =$ eigenvectors/eigenvalues of S .

Figure 12: Principal Geodesic Analysis Algorithm

In this project, PGA is believed to be useful for the shape analysis such as the analysis on thickness and the cross-sectional area of the sub-cortical brain regions. However, the PGA haven shown clinical significant on the subcortical region in this stage.

2.6 FreeSurfer

FreeSurfer is an open-source software that is created by Laboratory for Computational Neuroimaging for the MRI analysis and visualization. FreeSurfer provides complete solution for MRI processing including skull stripping, grey and white matter segmentation, cortical surface reconstruction, labelling regions on cortical surface and subcortical region, and measuring morphometric properties of the brain such as volume, surface area and cortical thickness [21].

In order to process the data, FreeSurfer require a high quality T1-weighted MRI data such T1 MPRAGE with approximately $1mm^3$ dimension and having excellent grey matter and white matter contrast. The outputs of the FreeSurfer normally in MGZ format which is a compressed MGH file. The MGZ file is similar to the Nifti file format as it also can store 4D data which are rows, columns, slices and frames. The MRI image can be construct by using the command *recon-all* command. This command will run all the process and create a subject folder “subject_id” in subject_directory and save all the data in the folder.

recon-all -all -i /path/to/input/data -s subject_id [47]

Basically, the FreeSurfer process can be divided into two processing stages which are Volumetric Processing Stages and Surface Processing Stages. In this thesis, we only focus on the volumetric processing stages since we only required the aseg.mgz which is one of the output that generated in volumetric processing stages for further analysis and processing. The table below show the steps of the volumetric processing stages and the output that generated in each step [21].

Table 1: Volumetric Processing Stages

Process	Step	Output
Volumetric Processing Stages	1. Motion Cor, Avg, Conform	orig.mgz
	2. Non-uniform inorm	nu.mgz
	3. Talairach transform computation	talairach/talairach.xfm
	4. Intensity Normalization 1	T1.mgz
	5. Skull Strip	Brainmask.mgz
	6. EM Register	

	7. CA Intensity Normalization	norm.mgz
	8. CA Non-linear Volumetric Registration	
	9. CA Label (Volumetric Labeling)	aseg.mgz
	10. Intensity Normalization 2	T1.mgz
	11. White matter segmentation	wm.mgz
	12. Edit WM With ASeg	
	13. Fill and cut	filled.mgz

The first step is to perform motion correction and averaging [48][47]. In this step, FreeSurfer will correct the small motion and average them together if there a multiple source volume. This step does not change the native resolution. After that, the conform process is perform by resample the source data to $256*256*256$ with $1mm^3$ resolution and the output of this step is name as orig.mgz. During the NU intensity correction, the non-uniformity T1-weighted MRI data is corrected and B1 bias field is removed to improve the accuracy of brain segmentation using MINC tools [47]. The bias-free data can be produced through an iterative process, four iteration are run by default [49].

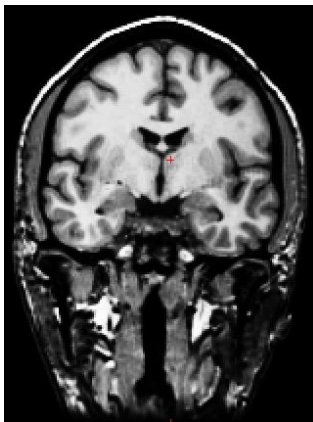


Figure 14 : orig.mgz [26]

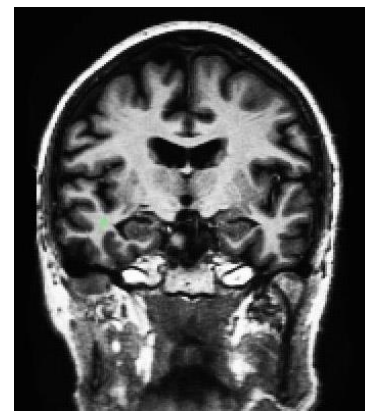


Figure 13 : nu.mgz [26]

Affine transform is computes to transform the orig volume to the MNI315 brain atlas by using MINC program during the talairach transform computation [50]. Next, the intensity normalization is performed on the orig volume and the output of this step is T1.mgz. In this step, fluctuations in the intensity is corrected. All voxel intensities are scaled so that the intensity of the white matter is 110 [47]. This step will be perform before and after the skull-strip.

All the non-brain tissues such as eyes, neck and bones are removed in the skull-strip step using skull-stripping algorithm [51]. After skull-stripping, the result is saved as Brainmask.mgz and left the brain tissues only.

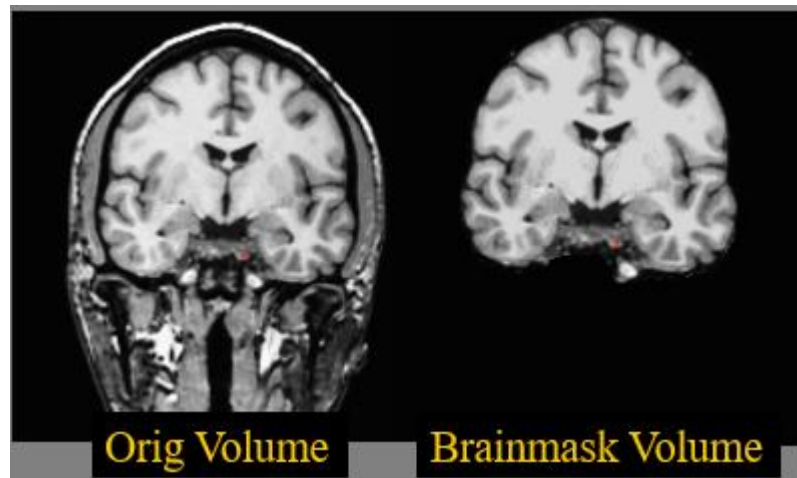


Figure 15: Before and After Skull Strip [26]

EM registration is similar with the talairach transform computation which the transform is computed to align the orig volume with the default atlas that can be found in the FreeSurfer. The volume file is then used to perform the automatic volume labelling. During this step, each of the voxels is labelled to a specific number and specific RGB value based on the location, intensity and neighborhood relationships. It is useful to determine the volumes of subcortical structures and easy for user to segment out the region of interest.

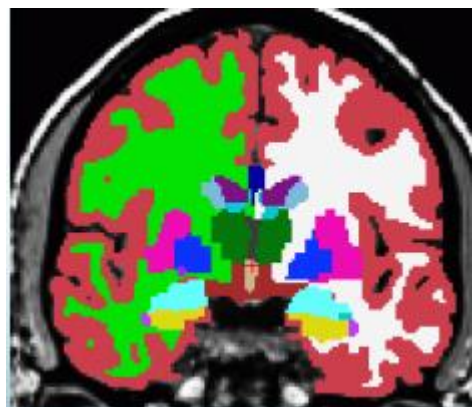


Figure 16 : Automatic Segmentation File (aseg.mgz) [26]

2.7 Spharm-pdm

Spharm-pdm is an automated set of algorithms that for statistical shape analysis based on the spherical harmonic representation which developed by Neuro Image Research and Analysis Laboratories, University of North Carolina. In other words, the Spharm-pdm is a parametric boundary description that represent the subject of spherical topology [52].

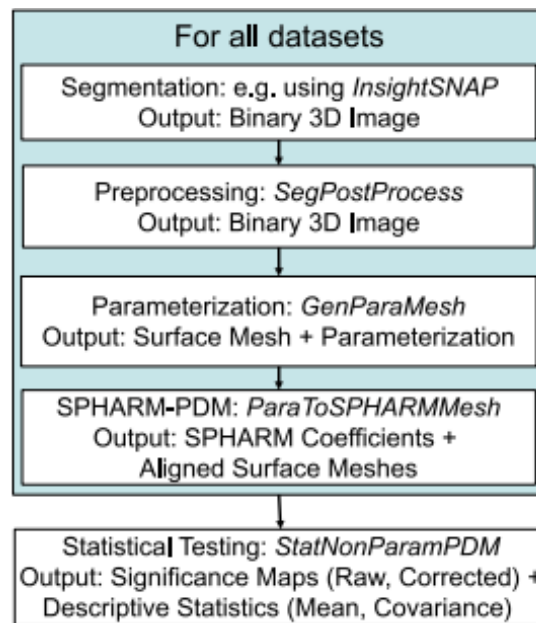


Figure 17 : Spharm-pdm Workflow [53]

The Spharm-pdm take 3d binary segmented data which in nifty or gipl format as an input. During the pre-processing step, heuristic methods is applied to make sure the spherical topology of the segmentation [53].The 3d voxel mesh is mapping on the sphere and minimize the angular distortion during the spherical parameterization step. Besides that, the ParaToSPHARMMesh is used to computed the Spharm-pdm shapre representation [53]. After that, the statistical testing will analysis the difference maps, significant maps, means surfaces and covariance matrix [53][54].

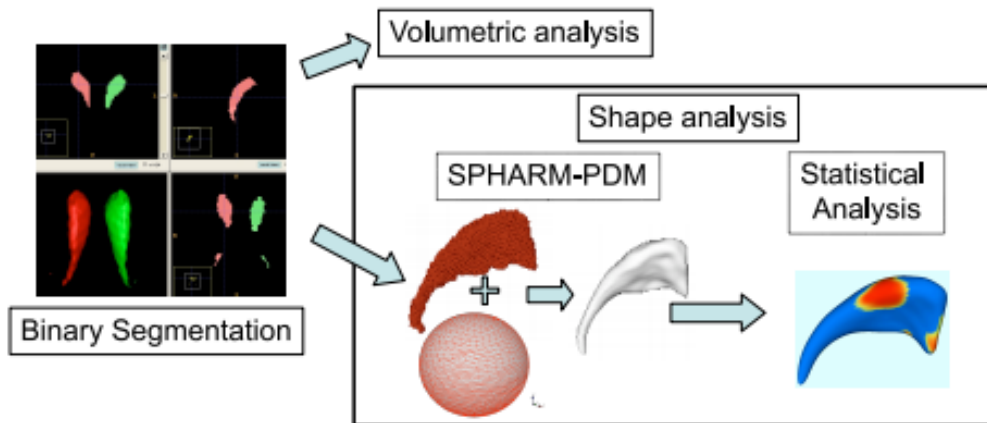


Figure 18 : Spharm-pdm shape analysis pipeline [53]

CHAPTER 3 METHODOLOGY

3.1 Research Methodology

This project is mainly to develop a visualisation tool for the brain morphometric analysis. The data that is used in this project is T1-weighted image which T1 flash and T1 MPRage image format. Approximately 20 normal control group data are collected from Midas100 [20]. The images are pre-processing by using an open source software FreeSurfer which is developed by Athinoula A.Martinos Center for Biomedical Imaging. FreeSurfer is a brain imaging software package that is useful in processing and analysis of brain structure based on the volume and surface-based analysis [21]. The FreeSurfer takes brain MRI data and generates labelled cortical surfaces and labelled cortical volumes. Run the command recon-all to process the T1-weighted image(\$IMAGE) and set the output name as \$SUBJECT. After the data has been processed, the output files stored at the file name \$SUBJECT.

```
recon-all -all -i $IMAGE -s $SUBJECT
```

The pair of hippocampus is then extracted using a defined algorithm written in python from the aseg.mgz file which is one of the output file generated from FreeSurfer. The processing time in this step might be long because 15 images of data need to be processed and the estimate runtime for each data in FreeSurfer takes approximately 1 day.

After the hippocampus is extracted, the volume of the hippocampus can be calculated by counting the number of voxel. The result is plotted in the histogram to observe the difference in the volume.

The output of the hippocampus segmentation need to be convert the format from nifti to STL mesh file using ITK-snap. The visualisation is created to visualise and compare between two subject. The visualisation tool can rotate, move and overlay two subject in order to compare the shape difference.

The boundary shape analysis and the medial shape analysis are used to analysis and compare the shape of the region of interest. The PCA algorithms is implemented with the visualization tools in order to show the first principal component of the

3.2 Project Activity

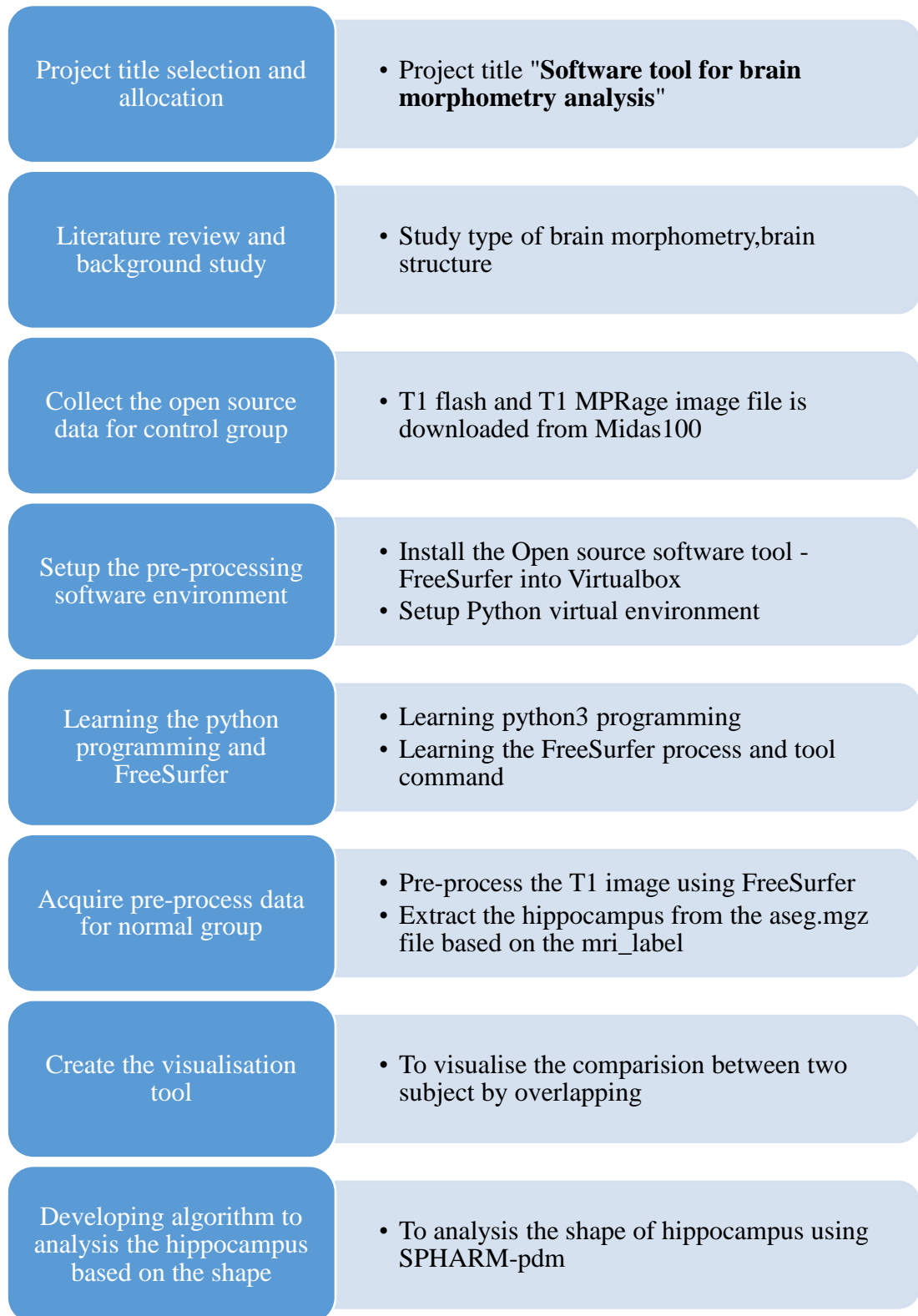


Figure 19: Project Activity Flow

3.3 Gantt Chart and Milestone of FYP

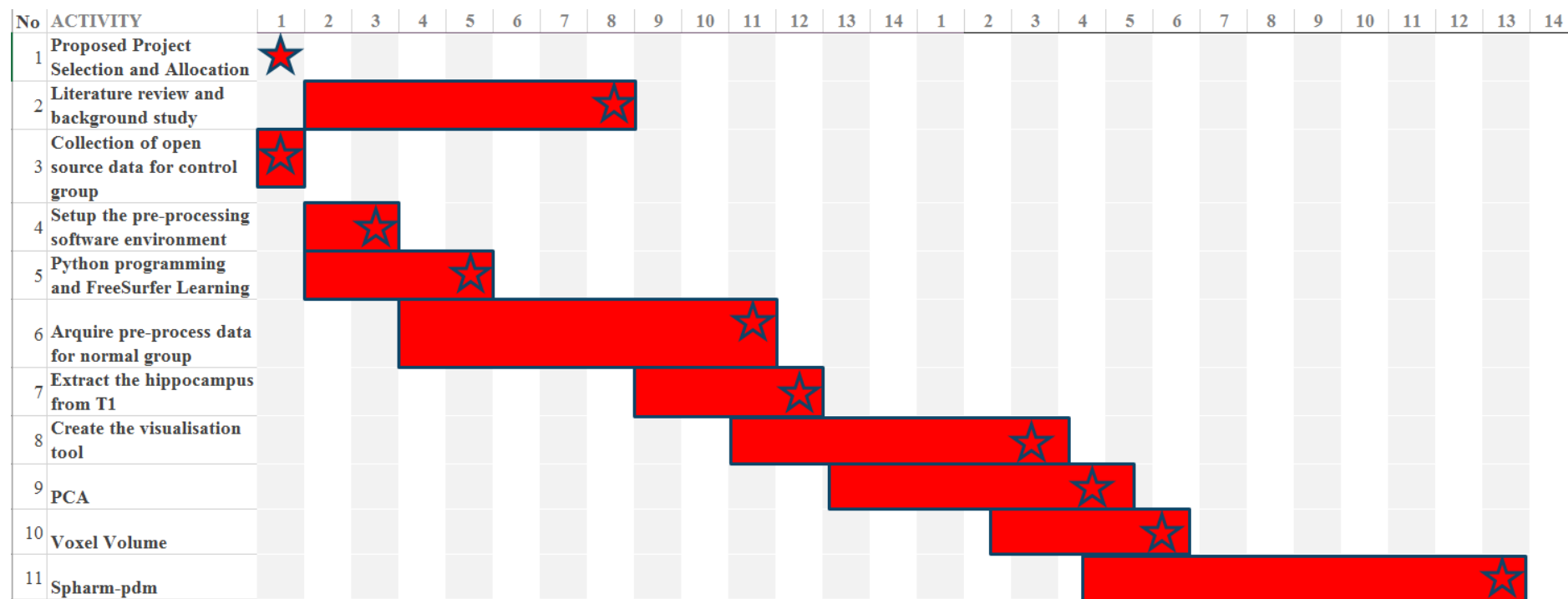


Figure 20: Gantt Chart for FYP

3.4 Data Acquisition

The T1 weighted MRI datasets which in MetaImages format were acquired from the open source database-Midas[20] to study and analysis the shape. The T1 weighted MRI datasets that used in this study were collected by the CASILab at University of North Carolina and distributed by the MIDAS at Kitware. Approximately 20 healthy control subjects (10 female and 10 male, range of age:19-55) are obtained [38]. The dimension of the T1-weighted MRI dataset is 176*256*176 and the voxel size is 1mm*1mm*1mm.The repetition time (TR) is 14 and the echo time(TE) is 7.7 with the flip angle 30⁰.

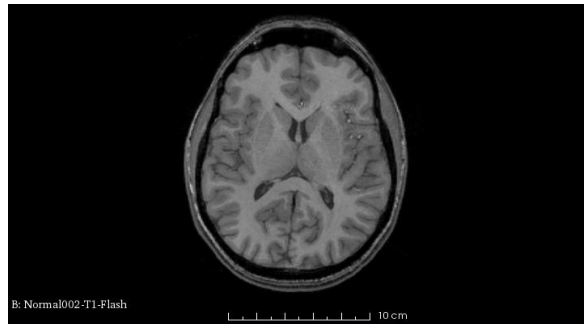


Figure 21: T1-weighted MRI (axial plane)



Figure 22 : T1-weighted MRI (sagittal plane)

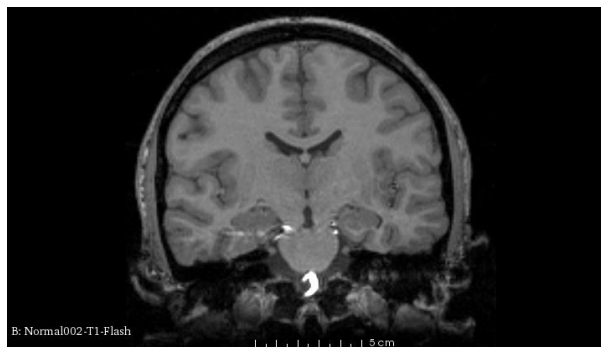


Figure 23 : T1-weighted MRI (coronal plane)

3.5 Data Pre-processing

The images are pre-processing by using an open source software FreeSurfer which is developed by Athinoula A.Martinou Center for Biomedical Imaging. FreeSurfer is a brain imaging software package that is useful in processing and analysis of brain structure based on the volume and surface-based analysis [21]. The FreeSurfer takes T1-weighted MRI data as an input and reconstruct a three-dimensional volume of the subject based on the MRI data.

In order to perform all the freesurfer reconstruction process, the command recon-all is used process the T1-weighted image(\$IMAGE) and set the output name as \$SUBJECT. After the data has been processed, the output files stored at the file name \$SUBJECT. It takes approximately one to finish the whole process for each subject.

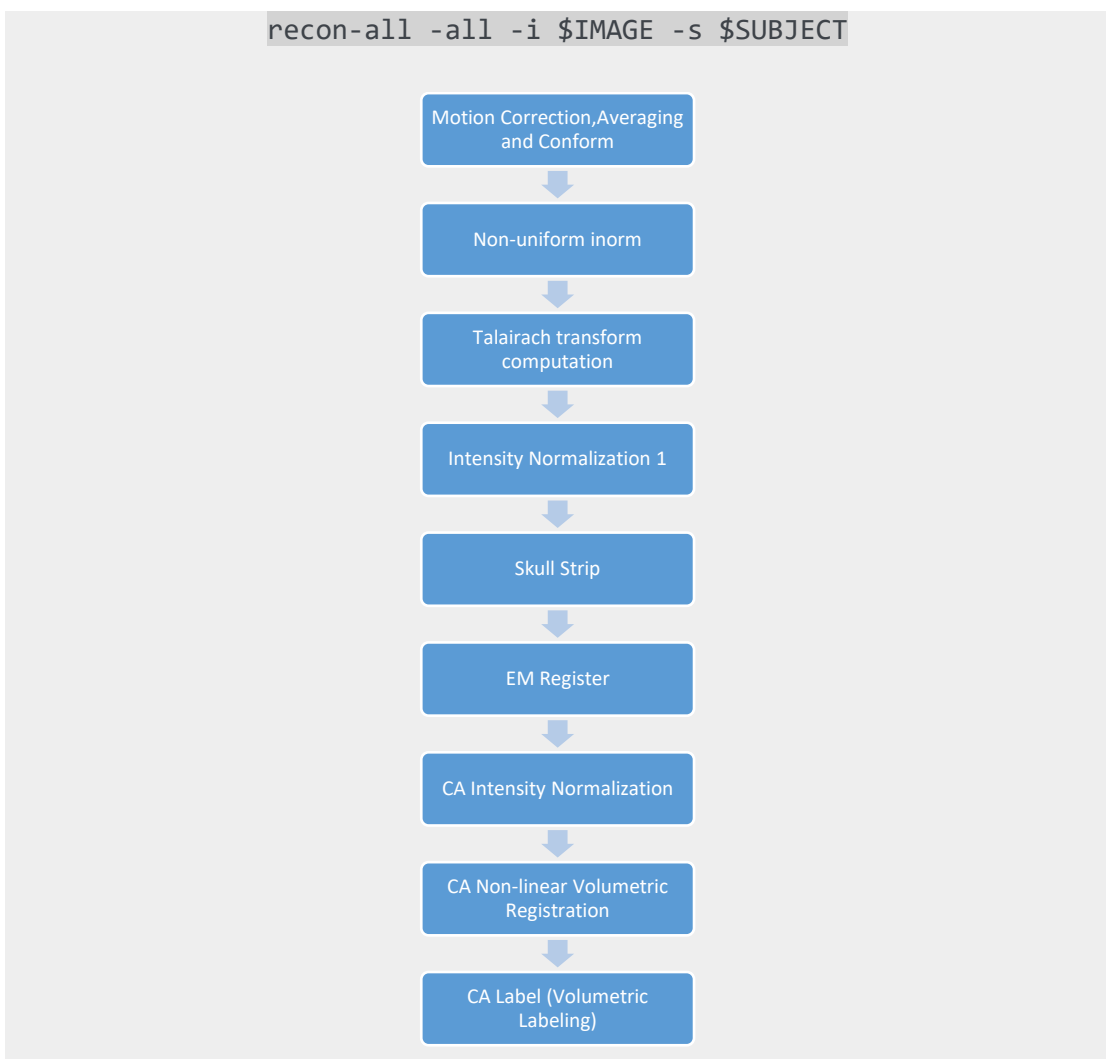


Figure 24 : Data Pre-processing Flow

The first stage of the FreeSurfer is to perform the motion artefact correction on the subject to correct for the small motion. Motion artifacts will affect the accuracy of the results[39]. After that, the FreeSurfer will resample the data and change the dimension into $265*265*265$ with $1mm^3$ voxel size. Then, skull strip process is performed which the non-brain tissues such as skull, eyes and ears are eliminated. Next ,the FreeSurfer perform the automatic Volume Labelling process which label the subcortical region based on the location and the intensity [40]. The output of this process (aseg.mgz) is then use for further analysis and process.

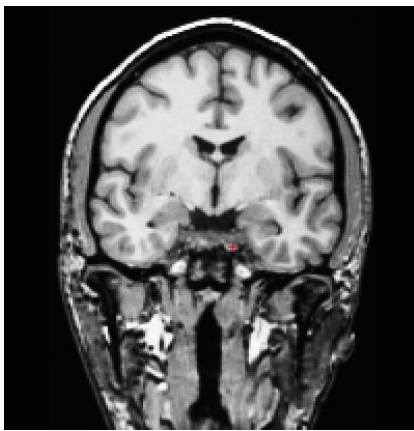


Figure 26 : Before Skull Strip

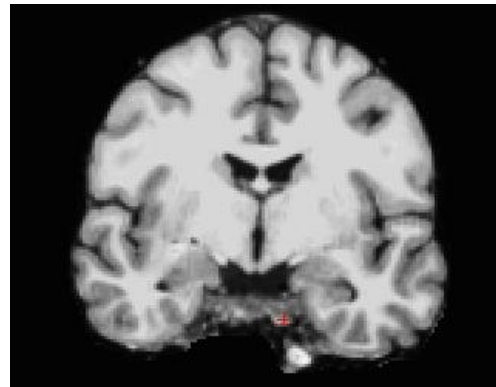


Figure 25 : After Skull Strip

3.6 Subcortical Segmentation

In order to compare a particular subcortical region, the segmentation process need to be done by extract the region of interest from the aseg.mgz file. Each of the subcortical region is label to a specific number which is easy for extract the region of interest. For example, the left hippocampus is been label as 17 while the right hippocampus is label as 53. Before the segmentation process is done, the aseg file need to convert into nifti format. The region of interest is segment out using a python script which set the region of interest into one else set to zero. The result is saved in nifti format and it can be consider as binary file. The result is then used for Spharm-pdm analysis and volume analysis.

3.7 Principal Component Analysis (PCA)

After the segmentation step, the output is used to perform the PCA analysis to compute the first three principal components. The PCA can be compute by using following steps. The PCA algorithms is then applied to the visualization tool to show the first principal component of the region of interest.

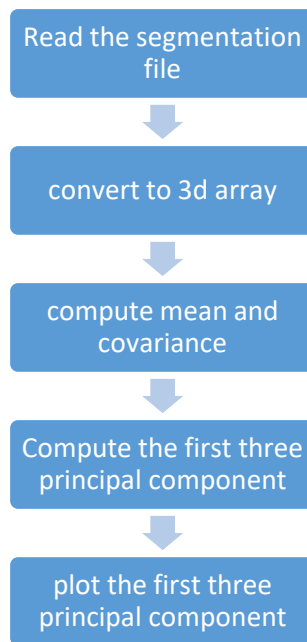


Figure 27 : PCA Flow

3.8 Spharm-pdm

The Spharm-pdm is used for boundary shape analysis and medial shape analysis. Spharm-pdm take the output of subcortical segmentation as an input. It only accepts the nifti file format and gipl file format. The 3d segmentation file must in binary format. Spharm-pdm allow user to run multiple data at the same time, so the input data path need to save in the csv file. The output directory need to be set by user and all the output from the Spharm-pdm will save in the folder. During post processed segmentation, the spacing parameter need to be set to determine the resolution of data. In this case, the spacing parameter is set 0.5mm for x, y and z-axis. In the ParaToSpharmMesh, the medial mesh option is selected, so that the Spharm-pdm will compute the medial axis of the data. The number of theta iteration and phi iteration is corresponding to the number of sample used to compute the medial mesh. After setting the parameter required, the Spharm-pdm can be run. Each of the data take approximately 10 min to complete.

Input File: PHARM_Tutorial_Data_July2015/SPHARM_Tutorial_Data_July2015/small_sample.csv

Randomize Inputs:

Output Directory: D:/SPHARM_Tutorial_Data_July2015/SPHARM_Tutorial_Data_July2015/fyp_ketum_4_5_1

Verbose mode:

Post Processed Segmentation

Overwrite:

Rescale:

sx: 0.5

sy: 0.5

sz: 0.5

Label Number:

Value: 1.00

Generate Mesh Parameters

Overwrite:

Number of Iterations: 1000

Parameters To SPHARM Mesh

Overwrite:

SubdivLevel value: 10

SPHARM Degree value: 15

Number of theta iterations: 100

Number of phi iterations: 100

Build the medial mesh:

Figure 28 : Spharm-pdm parameter

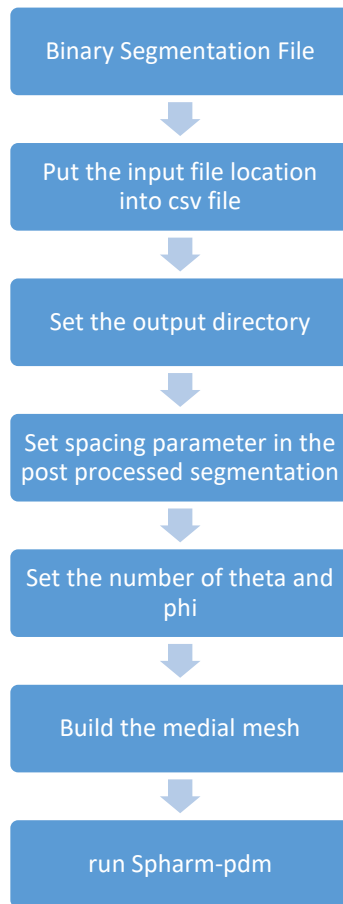


Figure 29: Spharm-pdm flowchart

CHAPTER 4 RESULTS AND DISCUSSION

4.1 Data Pre-processing

The normal group data is pre-processed using the open-source tool called FreeSurfer. T1 weighted image is used as the input of the FreeSurfer. In this project, aseg.mgz is the file that is required for further analysis. The aseg file consists of 40 subcortical regions and each of the subcortical region is labelled a specific number and colour. Figure 30 shows the aseg file, the region that colour in light green is right cerebral white matter with the label 41 which the region that in grey colour is brain stem with the label 16.

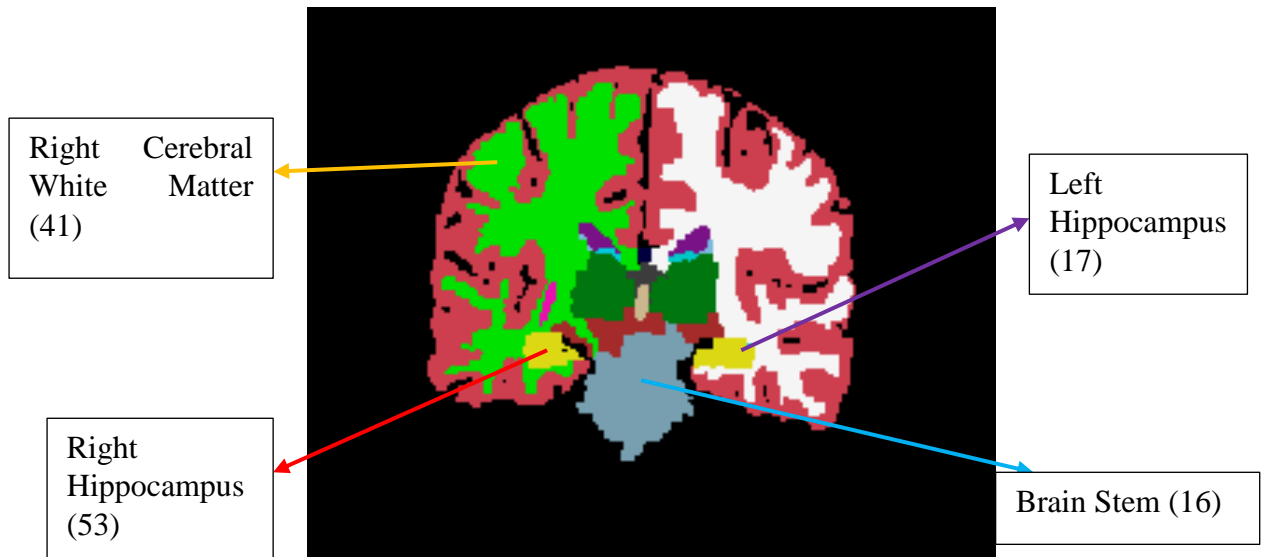


Figure 30: Snapshot of aseg file that show the label 41

4.2 Subcortical Segmentation

As stated in the scope of study, this project mainly concerns the subcortical region of hippocampus. So, a pair of hippocampus is identified in the pre-processing stage. After pre-processing, each part of the brain is assigned the labels to indicate different unique subcortical regions. To the left hippocampus of subject, the label is 17 while the right hippocampus is 53. To extract the hippocampus out from the brain, a python script is developed to set all the coordinates that have been labelled of 53 and 17 into 1 and else set into 0. Having binarizing the data, the image of a pair of hippocampus can be displayed in greyscale based on the '1' threshold. The output file is saved to 'nifti' format which can be used for further analysis. The figure below shows the hippocampus being extracted using the python script.

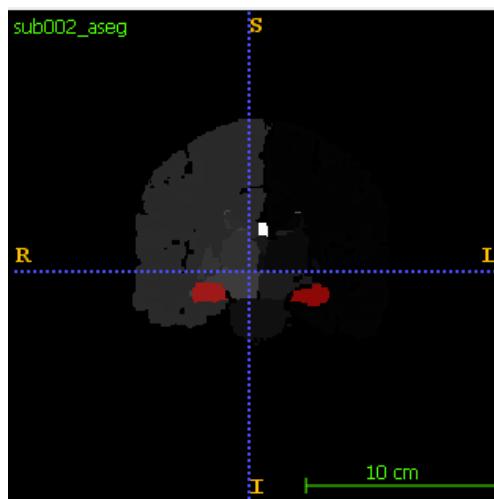


Figure 31: Hippocampus Segmentation (front view)

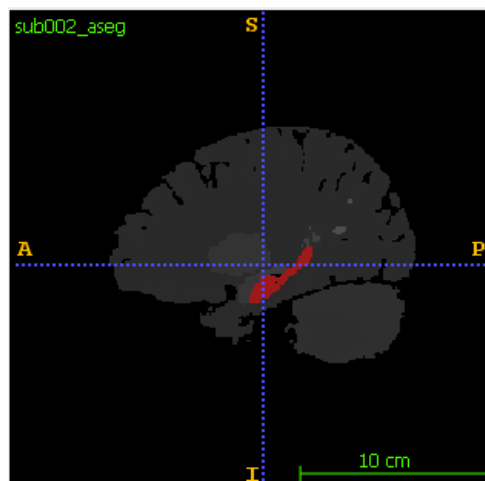


Figure 32: Hippocampus Segmentation (side view)

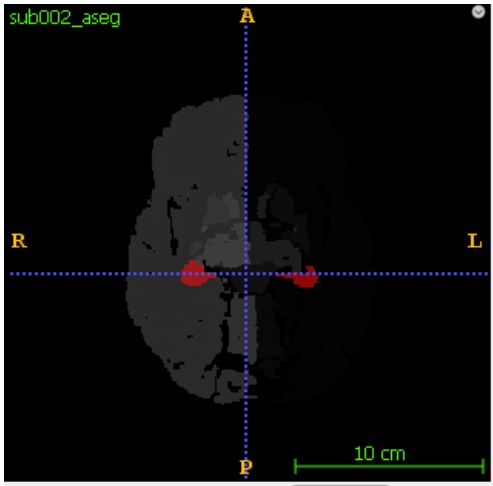


Figure 33: Hippocampus Segmentation (top view)

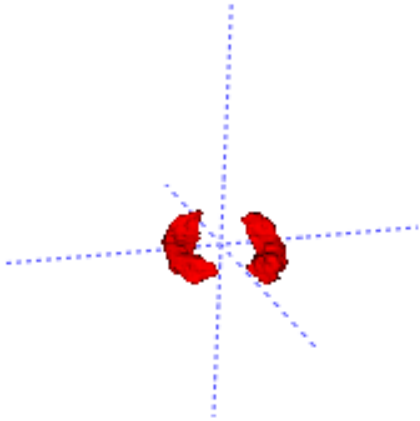


Figure 34: Hippocampus Segmentation (3d view)

4.3 Principal Component Analysis (PCA)

The PCA script is created to calculate the first three eigenvectors. The first eigenvector is the principal component of the data set with the most significance eigenvalue followed by second eigenvector and third eigenvector. The figure15 shows the first three eigenvectors of the hippocampus. The hippocampus is plotted in points because the image data is converted to numpy array before performing PCA. With the values of eigenvectors and the eigenvalues, they are useful when working with the VTK library. Based on the values obtained via the PCA algorithm, the visualization tool developed from the VTK library shows the most informative plane of the object by default for neuroimaging assessment.

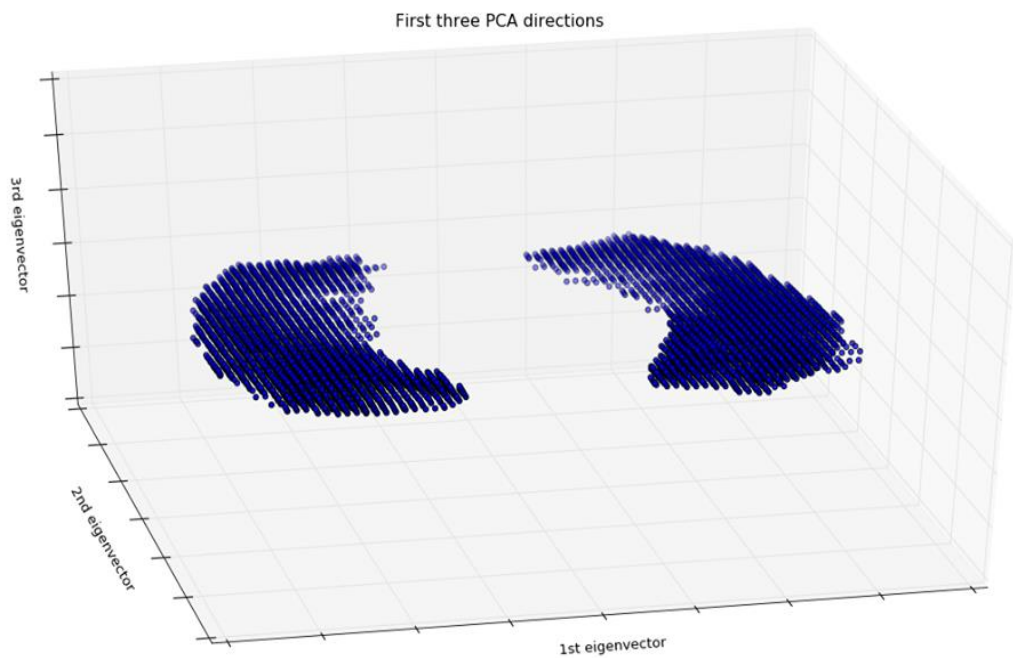
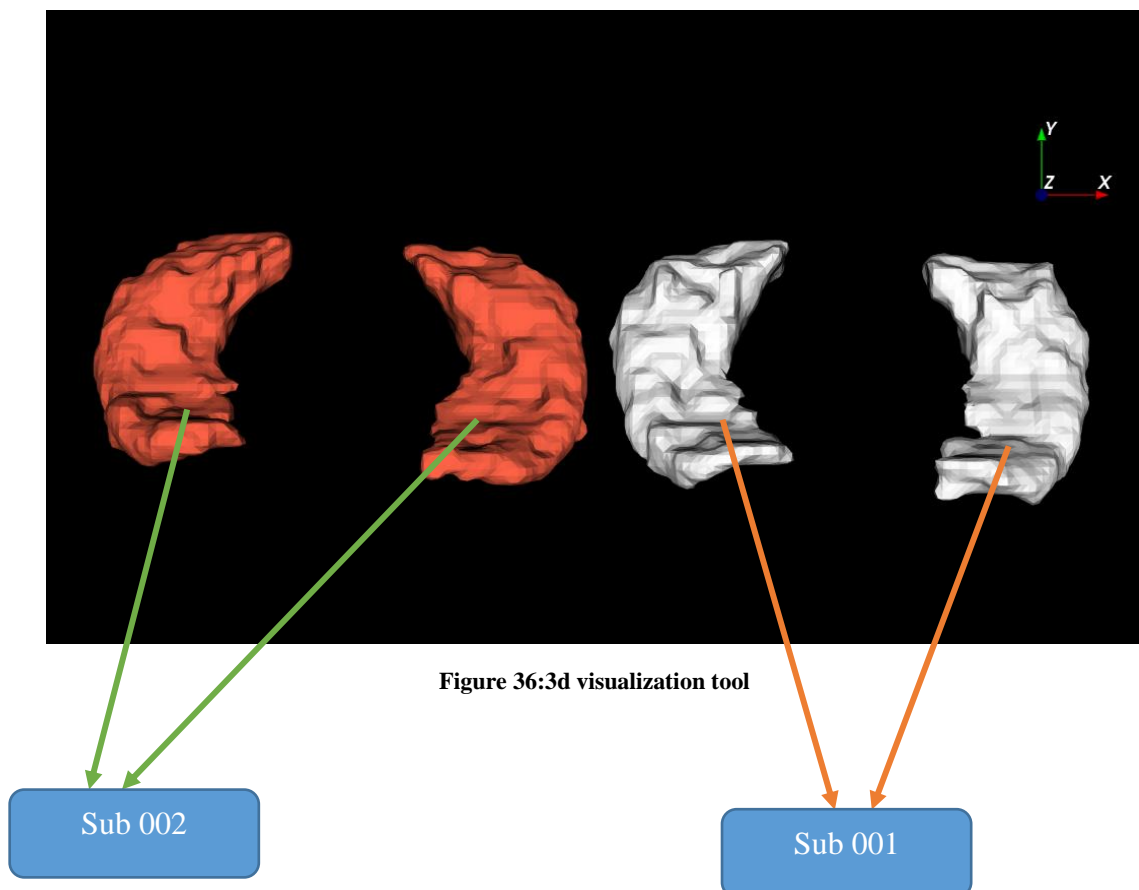


Figure 35: First Three PCA direction of hippocampus

4.4 3d Image Visualization

After the hippocampus is extracted, the output file is in nifty format. The next step is to overlay two sets of hippocampi of two different subjects together to give qualitative comparison in terms of shape changes. The output file from the hippocampus segmentation script is converted into STL mesh file. The VTK based python script is written to display two hippocampi. With the PCA algorithm, the most informative plane is shown by VTK for the visualization and comparison study.

The figure 36 shows the hippocampus of two normal groups, the grey one is the subject 'sub001' while the subject 'sub002' is shown in red colour. The visualization tool allows the user to render it. Besides that, the tool also allows user to move or drag the hippocampus overlapped with another, shown in figure 37 and figure 38.



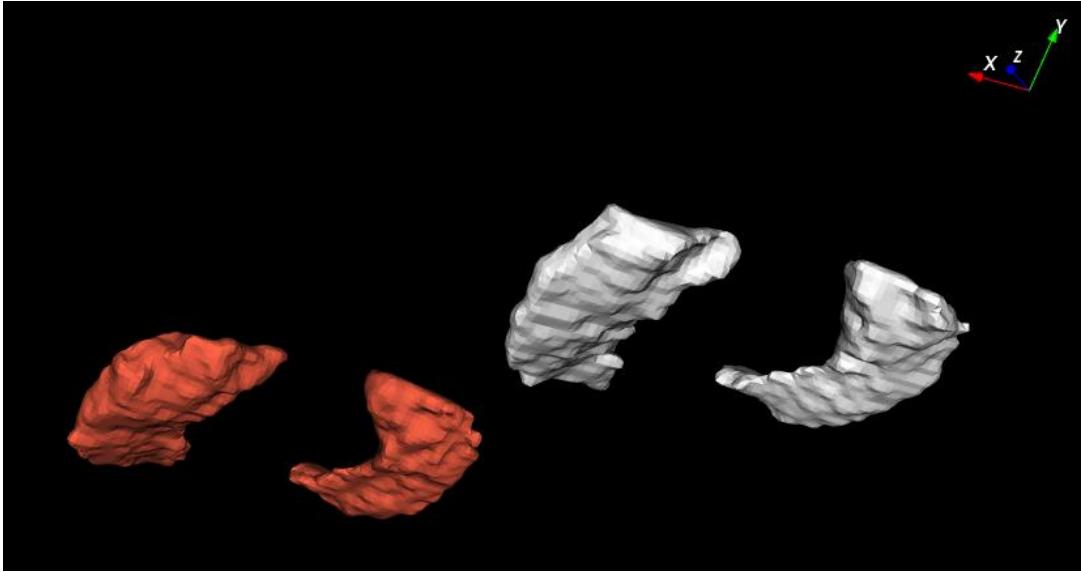


Figure 37: 3d visualization of two hippocampus with rotation

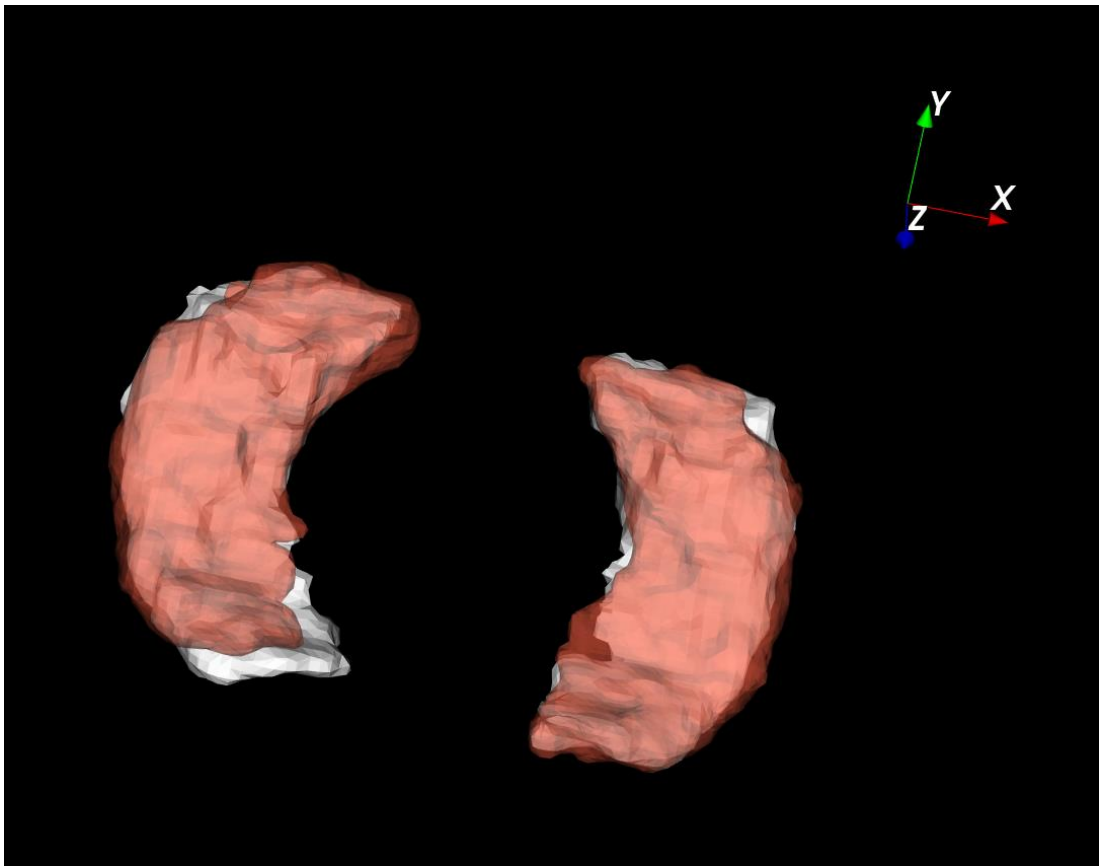


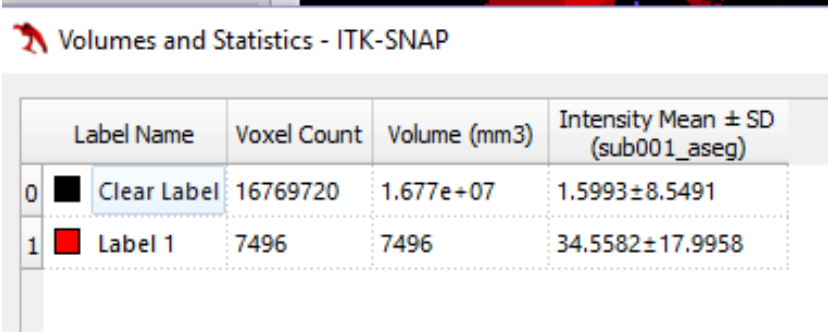
Figure 38:3d visualization with two hippocampus overlay

4.5 Voxel Volume

A python script is created to calculate the total number of voxel of the hippocampus. The size for each voxel box is 1mm*1mm*1mm. The input of this script is from the output of the hippocampus segmentation which is in binary file. The non-zero voxel is calculated and the volume of the hippocampus is calculated. The figure below shows the voxel count for normal group subject. From Figure 39, the voxel count for the hippocampus is 7496 voxels which means the voxel volume is 7496 mm^3 . The result that is obtained from the python script is similar with the ITK-Snap computation which indicates the result is accepted.

```
256
(256, 256, 256)
7496
```

Figure 39: Voxel count for normal group subject 001



	Label Name	Voxel Count	Volume (mm3)	Intensity Mean ± SD (sub001_aseg)
0	Clear Label	16769720	1.677e+07	1.5993±8.5491
1	Label 1	7496	7496	34.5582±17.9958

Figure 40: Voxel Count for normal group subject 001 (ITK-Snap)

The figure below shows the voxel volume of the left hippocampus and right hippocampus of 20 subject. The voxel volume of the sub001 is the smallest compared to other. This is because of the age is believed to be the root cause of the hippocampus atrophy in size for this subject001 who is a lady of age 55 [42]. On the other hands, the size of the subject014 who is a boy of age 19 is the largest. The underlying reason of this case is the hippocampus is considered largest at the puberty period of the development. Hippocampus generates many cells during puberty period compared to adulthood [41]. The size of the left hippocampus of majority of the subjects is largest compared to the right. This is deduced that the larger size of the left hippocampus is due to most of the subjects are right-handed.

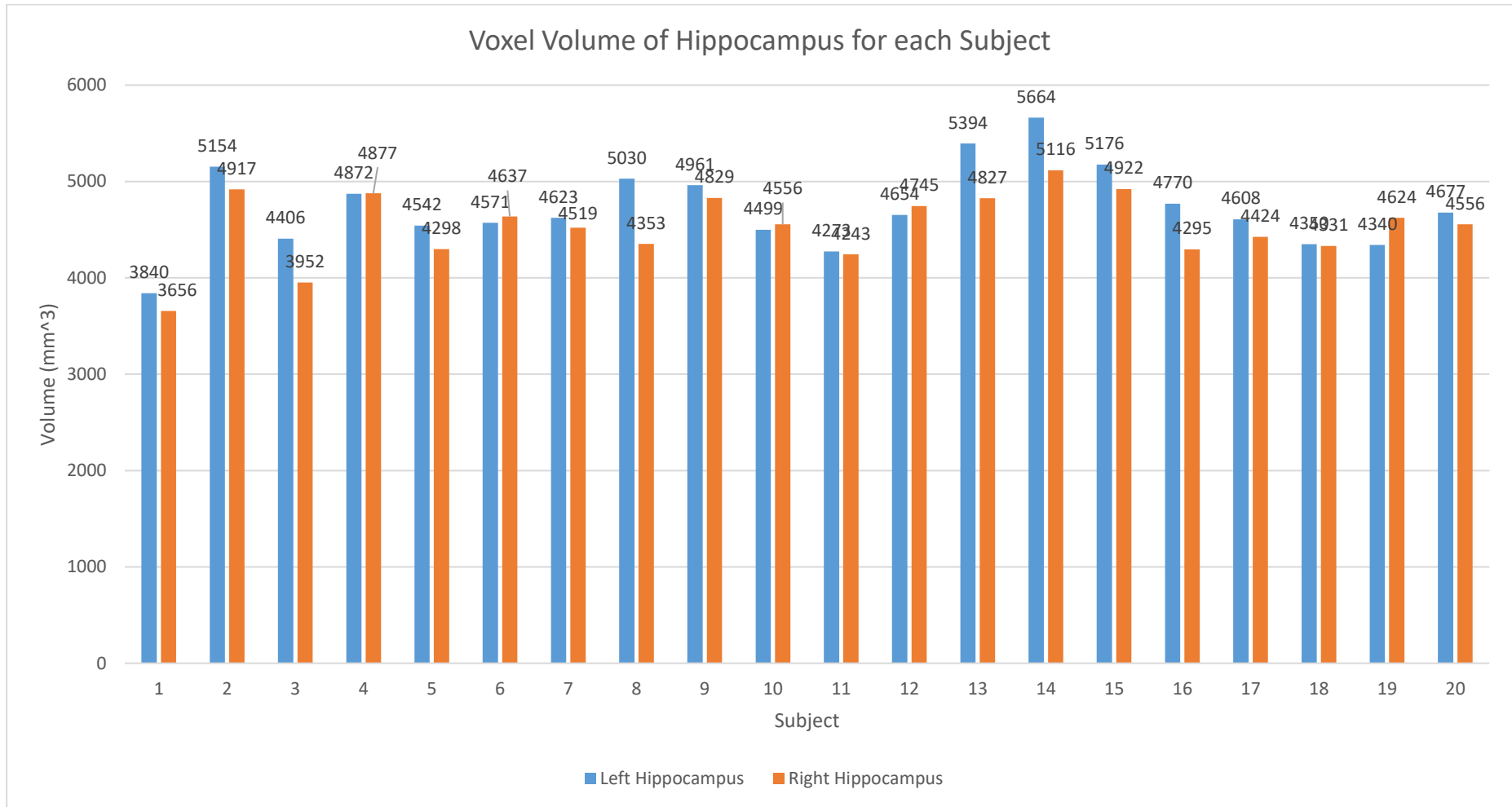


Figure 41 : Voxel volume of hippocampus for each subject

4.6 Boundary Shape Analysis via SPHARM

The boundary shape analysis with spherical harmonics SPHARM is adopted to localize any shape deformation in hippocampus. Modelling the surface of each hippocampus with the SPHARM requires three possessing pipeline, (1) Spherical Parametrization, (2) SPHARM expansion, and (3) SPHARM registration. Through SPARM, at every boundary point of the surface of the hippocampal subfield, a distance map color-coded with RGB values significantly allows locating any shape differences between the subject group and the template object.

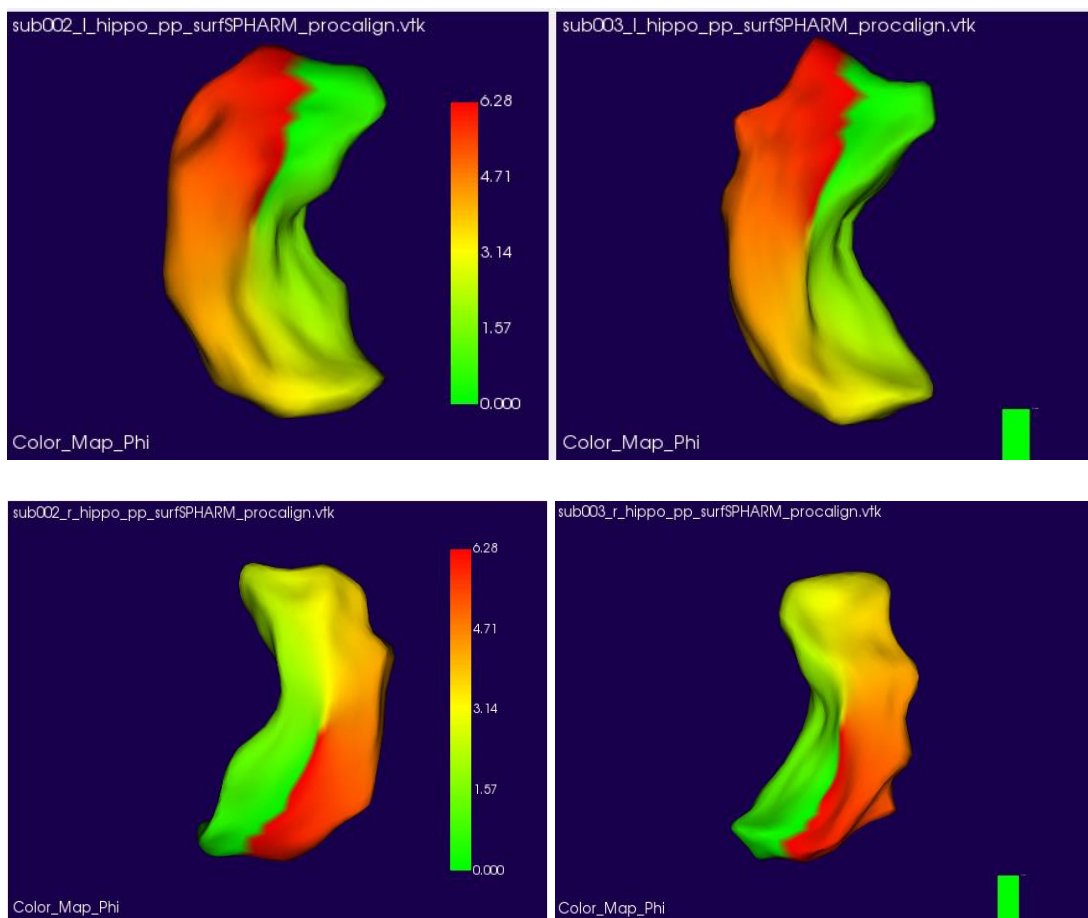


Figure 42 : Boundary Shape Analysis of sub002 and sub003(Top: Left hippocampus) (Bottom: Right hippocampus)

The result of the SPHARM illustrated in the two figures above describes the magnitude of difference as a colormap for the left hippocampal subfield of the subject_002 and the subject_003 compared with the template object. Obviously as the colormap describes, the green color of both of the subject_002 and the subject_003 indicates there is 0mm difference compared to the template at their left tail region. As the color

approaches to red, it indicates the shape between the subjects exhibits increasing large difference. The left visualization of the hippocampus of subject_002 is red for his right tail region, similar goes to the hippocampus of subject_003. This denotes that there exists the shape difference of 0.28mm around the red regions of both the subjects, compared between the subjects to the template, and between the subject_002 and subject_003. The colour of both hippocampus is almost similar due to both subject is under healthy control. So, the shape of the both subject is almost same.

4.7 Medial Shape Analysis

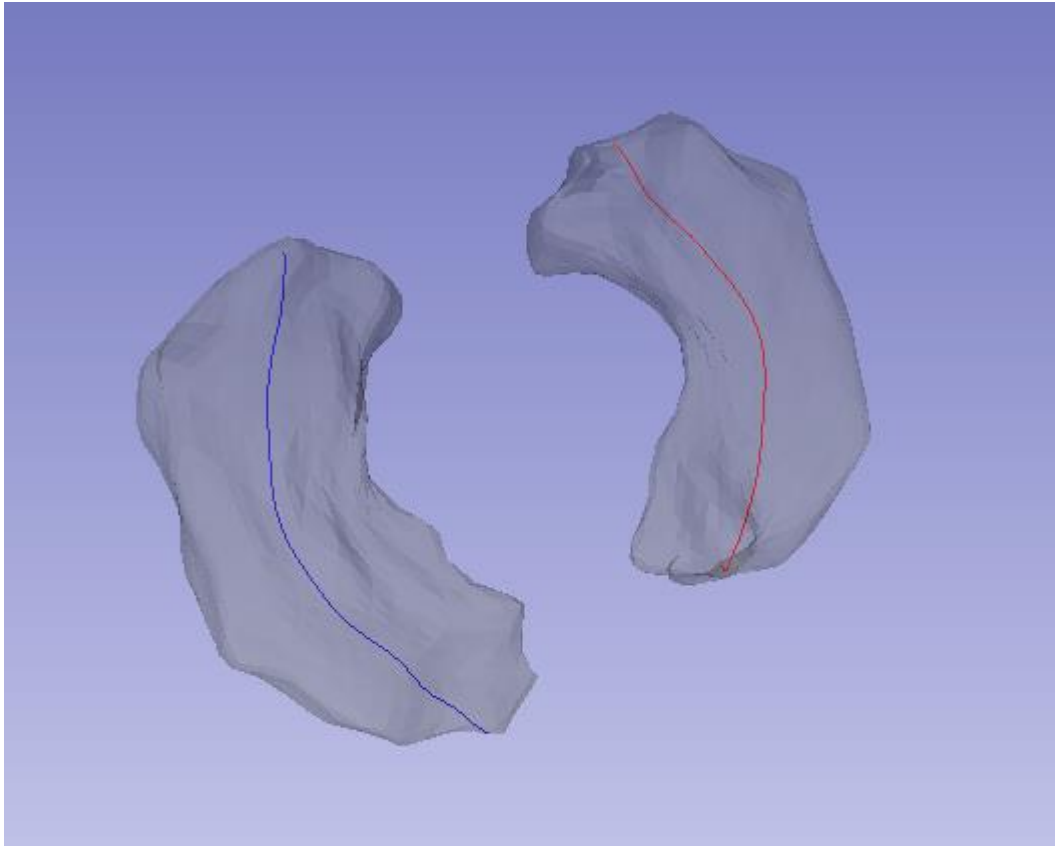


Figure 43 : Medial shape analysis of sub004

Unlike boundary shape analysis, the medial shape analysis is to provide the center local position of the hippocampal subfield. This approach is significant for describing the correspondence between points of two hippocampal shape. As the result of red and blue line computed to represent the left and the right medial axis of the hippocampus belong to the subject_004, the medial axis lines is quite symmetrical to each other. Another usefulness based on the sampled medial representation is that it allows the hippocampus model comparison by overlapping two medial axis of two subjects to each other. It ensures the correspondence of the placement of two objects in visualization and image analysis.

CHAPTER 6 CONCLUSION AND FUTURE WORK

Volume changes in region of interest is an intuitive feature of recognizing the atrophy or dilation of the subcortical regions of brain, caused by diseases. However, the structural changes at the location of the region of interests do not reflect the volume measurement. Hence, it does not permit quantitative analysis. So, the shape analysis of SPHARM-PDM is used together with the developed volume measurement algorithm in this thesis.

In this project, visualization software tool that is in easy to use format is developed for the clinicians to compare the brain region morphometry between the individual patients and normal group databases. In order to perform the brain morphometry analysis, the T1 image need to be pre-processed and the region of interest is extracted from the entire brain. After the data pre-processing stage is completed, the hippocampus is segmented based on the assigned label of 17 and 54. The GUI for 3d visualization is created and allow users to rotate and move the hippocampus. The PCA algorithm is developed and is informative for the visualization tool. The voxel volume of the hippocampus is calculated. The result is identical to the result presented by ITK Snap, which is a popular neuroimaging examination tool. The medial shape analysis and boundary shape analysis is carried out with SPHARM-PDM. The

The future work can be done by combining all the scripts together to make a complete software tool. The visualization tool can be enhanced by adding more features such as allowing users to add more subject and able to reset the hippocampus into the default original position. Besides that, other morphometry parameter such as subcortical thickness and orientation can be considered for future development. In a nutshell, brain morphometry studied across the healthy subject and the patient subject is carried up. Their hippocampi are observed and compared in the developed visualization tool. To analyse any unusual shape changes, SPAHRM-PDM used.

REFERENCES

- [1] Babb, T. (1987). Pathological findings in epilepsy. Surgical treatment of the epilepsies, 511-540.
- [2] FALCONER, M. A., SERAFETINIDES, E. A., & CORSELLIS, J. N. (1964). Etiology and pathogenesis of temporal lobe epilepsy. Archives of neurology, 10(3), 233-248.
- [3] Healthline Medical Team. (2015). Body Maps. Retrieved October 12,2016, from <http://www.healthline.com/human-body-maps/brain>
- [4] Stroke Education. (n.d.). Brain stem. Retrieved October 12,2016, from <http://www.strokeeducation.info/brain/brainstem/>
- [5] Human brain. (n.d.). In *Wikipedia, The Free Encyclopedia*. Retrieved October 12, 2016, from https://en.wikipedia.org/w/index.php?title=Human_brain&oldid=743695153
- [6] Ball, M., Hachinski, V., Fox, A., Kirshen, A., Fisman, M., Blume, W., . . . Merskey, H. (1985). A new definition of Alzheimer's disease: a hippocampal dementia. *The Lancet*, 325(8419), 14-16.
- [7] Mandal.A. (n.d.). "What is the Hippocampus?" *News Medical Life Sciences*. Retrieved October 12,2016, from <http://www.news-medical.net/health/Hippocampus-What-is-the-Hippocampus.aspx>
- [8] Brain morphometry. (n.d.). In *Wikipedia, The Free Encyclopedia*. Retrieved October 13, 2016, from https://en.wikipedia.org/w/index.php?title=Brain_morphometry&oldid=737273925
- [9] Lam, P. (2016, February 19). "MRI Scans: How Do They Work?." *Medical News Today*. Retrieved October 15, 2016, from <http://www.medicalnewstoday.com/articles/146309.php>.
- [10] Magnetic resonance imaging. (n.d.). In *Wikipedia, The Free Encyclopedia*. Retrieved October 15, 2016, from

https://en.wikipedia.org/w/index.php?title=Magnetic_resonance_imaging&ol did=744402818

- [11] Ashburner, J. & Friston, K. (2004) . Chapter 36 - Morphometry. *Human Brain Function (Second Edition)* (pp. 707-722). Burlington: Academic Press.
- [12] Mechelli, A., Price, C. J., Friston, K. J., & Ashburner, J. (2005). Voxel-based morphometry of the human brain: methods and applications. *Current medical imaging reviews*, 1(2), 105-113.
- [13] Ashburner, J., & Friston, K. J. (2000). Voxel-based morphometry—the methods. *Neuroimage*, 11(6), 805-821.
- [14] Honea, R., Crow, T. J., Passingham, D., & Mackay, C. E. (2005). Regional deficits in brain volume in schizophrenia: a meta-analysis of voxel-based morphometry studies. *American Journal of Psychiatry*, 162(12), 2233-2245.
- [15] Ashburner, J., Hutton, C., Frackowiak, R., Johnsrude, I., Price, C., & Friston, K. (1998). Identifying global anatomical differences: deformation-based morphometry. *Human brain mapping*, 6(5-6), 348-357.
- [16] Chung, M., Worsley, K., Paus, T., Cherif, C., Collins, D., Giedd, J., . . . Evans, A. (2001). A unified statistical approach to deformation-based morphometry. *Neuroimage*, 14(3), 595-606.
- [17] Tu, P.-C., Chen, L.-F., Hsieh, J.-C., Bai, Y.-M., Li, C.-T., & Su, T.-P. (2012). Regional cortical thinning in patients with major depressive disorder: a surface-based morphometry study. *Psychiatry Research: Neuroimaging*, 202(3), 206-213.
- [18] Le Bihan, D., Mangin, J. F., Poupon, C., Clark, C. A., Pappata, S., Molko, N., & Chabriet, H. (2001). Diffusion tensor imaging: concepts and applications. *Journal of magnetic resonance imaging*, 13(4), 534-546.
- [19] Bell-McGinty, S., Butters, M. A., Meltzer, C. C., Greer, P. J., Reynolds III, C. F., & Becker, J. T. (2002). Brain morphometry abnormalities in geriatric depression: long-term neurobiological effects of illness duration. *American Journal of Psychiatry*.

- [20] Midas. (n.d.). Designed Database of MR Brain Images of Healthy Volunteers. Retrieved from 2016, September 28 from <http://www.insight-journal.org/midas/community/view/21>
- [21] FreeSurfer. (n.d.). Retrieved 2016, September 30 from <https://surfer.nmr.mgh.harvard.edu/fswiki>
- [22] Shlens, J. (2014). A tutorial on principal component analysis. arXiv preprint arXiv:1404.1100.
- [23] Smith, L. I. (2002). A tutorial on principal components analysis. Cornell University, USA, 51, 52.
- [24] Seguy, V., & Cuturi, M. (2015). Principal geodesic analysis for probability measures under the optimal transport metric. Paper presented at the Advances in Neural Information Processing Systems.
- [25] Fletcher, P. T., Lu, C., Pizer, S. M., & Joshi, S. (2004). Principal geodesic analysis for the study of nonlinear statistics of shape. *IEEE transactions on medical imaging*, 23(8), 995-1005.
- [26] Sommer, S., Lauze, F., Hauberg, S., & Nielsen, M. (2010). Manifold valued statistics, exact principal geodesic analysis and the effect of linear approximations. Paper presented at the European Conference on Computer Vision.
- [27] FreeSurferColorLUT. (2010). Retrieved 2016, September 30 from <https://surfer.nmr.mgh.harvard.edu/fswiki/FsTutorial/AnatomicalROI/FreeSurferColorLUT>
- [28] Joseph J, Warton C, Jacobson SW, Jacobson JL, Molteno CD, Eicher A, Marais P, Phillips OR, Narr KL, Meintjes EM (2014): Three-dimensional surface deformation-based shape analysis of hippocampus and caudate nucleus in children with fetal alcohol spectrum disorders. *Hum Brain Mapp* 35:659–672.
- [29] Kim S.-G, Chung MK, Schaefer SM, van Reekum C, Davidson RJ (2012): Sparse shape representation using the laplace-beltrami eigenfunctions and its application to modeling subcortical structures. In: *IEEE Workshop on IEEE*

Workshop on Mathematical Methods in Biomedical Image Analysis (MMBIA), 2012. Breckenridge, CO: IEEE, pp 25–32.

- [30] Kristin L. Bigos, Ahmad R. Hariri, Daniel R. Weinberger (2015). *Neuroimaging Genetics: Principles and Practices*. Oxford University Press. p. 157.
- [31] Cosgrove, KP; Mazure CM; Staley JK (2007). "Evolving knowledge of sex differences in brain structure, function, and chemistry". *Biol Psychiat*. 62 (8): 847–55.
- [32] "Neuron." *The Gale Encyclopedia of Science*, edited by K. Lee Lerner and Brenda Wilmoth Lerner, 4th ed., vol. 4, Gale, 2008, pp. 2960–2963.
- [33] Kandel, ER; Schwartz JH; Jessel TM (2000). *Principles of Neural Science*. McGraw-Hill Professional. p. 324.
- [34] Bin He (2013). *Neural Engineering*. Springer Science & Business Media. pp. 9–10.
- [35] Sciences, Sandra Ackerman for the Institute of Medicine, National Academy of (1992). *Discovering the brain*. Washington, D.C.: National Academy Press. pp. 22–25.
- [36] Standring, S., Ellis, H., Healy, J., & Williams, A. (2008). *Grays Anatomy 40th Edition. Anatomical Basis Of Clinical Practice*, Churchill Livingstone, London, 40, 415.
- [37] Hopes. (2010). *Dementia in Huntington's Disease*. Retrieved April 7, 2017, from http://web.stanford.edu/group/hopes/cgi-bin/hopes_test/dementia-in-huntingtons-disease/
- [38] Bullitt E, Zeng D, Gerig G, Aylward S, Joshi S, Smith JK, Lin W, Ewend MG (2005) Vessel tortuosity and brain tumor malignancy: A blinded study. *Academic Radiology* 12:1232-1240

- [39] Fischl B., Dale A. M. (2000). Measuring the thickness of the human cerebral cortex from magnetic resonance images. *Proc. Natl. Acad. Sci. U.S.A.* 97, 11050–11055. 10.1073/pnas.200033797
- [40] Dale A. M., Fischl B., Sereno M. I. (1999). Cortical surface-based analysis. I. segmentation and surface reconstruction. *Neuroimage* 9, 179–194. 10.1006/nimg.1998.0395
- [41] Curlik, D. M., DiFeo, G., & Shors, T. J. (2014). Preparing for adulthood: thousands upon thousands of new cells are born in the hippocampus during puberty, and most survive with effortful learning. *Frontiers in neuroscience*, 8, 70.
- [42] Erickson, K. I., Prakash, R. S., Voss, M. W., Chaddock, L., Heo, S., McLaren, M., . . . Woods, J. A. (2010). Brain-derived neurotrophic factor is associated with age-related decline in hippocampal volume. *Journal of Neuroscience*, 30(15), 5368-5375.
- [43] MedlinePlus Trusted Health Information for You. (n.d.). MRI. Retrieved March 16,2017 from <https://medlineplus.gov/ency/article/003335.htm>
- [44] WebMD. (n.d.). Magnetic Resonance Imaging(MRI). Retrieved March 16,2017 from <http://www.webmd.com/a-to-z-guides/magnetic-resonance-imaging-mri#1>
- [45] Wilkinson ID, Graves MJ. Magnetic resonance imaging. In: Adam A, Dixon AK, Gillard JH, Schaefer-Prokop CM, eds. *Grainger & Allison's Diagnostic Radiology*. 6th ed. New York, NY: Elsevier; 2015:chap 5.
- [46] Basic proton MR imaging. (n.d.). Retrieved April 15, 2017, from <http://www.med.harvard.edu/aanlib/basicsMR.html>
- [47] recon-all.(n.d.). Retrieved on April 10, 2017 from <https://surfer.nmr.mgh.harvard.edu/fswiki/recon-all>
- [48] McCarthy, C. S., Ramprashad, A., Thompson, C., Botti, J.-A., Coman, I. L., & Kates, W. R. (2015). A comparison of FreeSurfer-generated data with and without manual intervention. *Frontiers in neuroscience*, 9.

- [49] Zheng, W., Chee, M. W., & Zagorodnov, V. (2009). Improvement of brain segmentation accuracy by optimizing non-uniformity correction using N3. *Neuroimage*, 48(1), 73-83.
- [50] Collins, DL, Neelin, P., Peters, TM, and Evans, AC. (1994) Automatic 3D Inter-Subject Registration of MR Volumetric Data in Standardized Talairach Space, *Journal of Computer Assisted Tomography*, 18(2) p192-205, 1994 PMID: 8126267; UI: 94172121
- [51] Ségonne, F., Dale, A. M., Busa, E., Glessner, M., Salat, D., Hahn, H. K., & Fischl, B. (2004). A hybrid approach to the skull stripping problem in MRI. *Neuroimage*, 22(3), 1060-1075.
- [52] C. Brechbühler, G. Gerig, and O. Kübler, "Parametrization of closed surfaces for 3-D shape description," *Computer Vision, Graphics, Image Processing: Image Understanding*, vol. 61, pp. 154–170, 1995.
- [53] Styner, M., Oguz, I., Xu, S., Brechbühler, C., Pantazis, D., Levitt, J. J., . . . Gerig, G. (2006). Framework for the statistical shape analysis of brain structures using SPHARM-PDM. *The insight journal*(1071), 242.
- [54] Styner, M., Lieberman, J. A., Pantazis, D., & Gerig, G. (2004). Boundary and medial shape analysis of the hippocampus in schizophrenia. *Medical image analysis*, 8(3), 197-203.
- [55] Central nervous system. (2017). In *Wikipedia, The Free Encyclopedia*. Retrieved April 15, 2017, from https://en.wikipedia.org/wiki/Central_nervous_system
- [56] Anatomy of the Brain.(n.d.). *Mayfield Brain & Spine*. Retrieved April 15,2017 from <http://www.mayfieldclinic.com/PE-AnatBrain.htm>
- [57] Basic Principles of MR Imaging.(n.d.). Retrieved April 15,2017 from <http://spinwarp.ucsd.edu/neuroweb/Text/br-100.htm>
- [58] Image contrast.(n.d.). Retrieved April 15, 2017 from <https://mrimaster.com/characterise%20physics.html>

APPENDICES

Appendix A : Subcortical Segmentation

```
from medpy.io import load,header,save
from medpy.filter import otsu
import matplotlib.pyplot as plt

filename = 'sub025_aseg.nii.gz'
image_data, image_header = load(filename)
mrishape = image_data.shape
#print image_data
print mrishape
#print image_header
mrivoxspacing = header.get_pixel_spacing(image_header)
mrioffset = header.get_offset(image_header)
#thr_image_data = (image_data == 53)
thr_image_data = (image_data == 17)
#thr_image_data = (image_data == 53) + (image_data==17) # Extract the
hippocampus (17 is left, 53 is right)
#print "thr_image",thr_image_data[0]
plt.imshow(thr_image_data[:,128,:])
plt.colorbar()
plt.show()

outpath = 'sub025_1_hippo.nii.gz'
save(thr_image_data, outpath, image_header)
```

Appendix B : PCA

```
import matplotlib.pyplot as plt
from mpl_toolkits.mplot3d import Axes3D
from sklearn import datasets
from sklearn.decomposition import PCA
import numpy as np
import nibabel as nib

img = nib.load("sub001_output.nii.gz")
data = img.get_data()
print(len(data))

#print data
print data.shape
#print data[0][1]

datalist=[]
for i in range(0,data.shape[0]):
    for j in range(0,data.shape[1]):
        for k in range(0,data.shape[2]):
            if data[i][j][k] == 1:
                datalist.append([i,j,k])

print len(datalist)
N=len(datalist)
img_data = np.asarray(datalist)

# To get a better understanding of interaction of the dimensions
# plot the first three PCA dimensions
fig = plt.figure(1, figsize=(8, 6))
ax = Axes3D(fig, elev=-150, azim=110)
X_reduced = PCA(n_components=3).fit_transform(img_data)
#ax.scatter(X_reduced[:, 0], X_reduced[:, 1], X_reduced[:, 2],
#           cmap=plt.cm.Paired)
ax.scatter(X_reduced[:, 0],X_reduced[:, 1], cmap=plt.cm.Paired)
ax.set_title("First three PCA directions")
ax.set_xlabel("1st eigenvector")
ax.w_xaxis.set_ticklabels([])
ax.set_ylabel("2nd eigenvector")
ax.w_yaxis.set_ticklabels([])
ax.set_zlabel("3rd eigenvector")
ax.w_zaxis.set_ticklabels([])

plt.show()
```

Appendix C : Visualization Tools

```
import vtk
from vtk.util.colors import tomato

# create source 1
filename = "hippo1.stl"
filename2="hippo2.stl"

reader = vtk.vtkSTLReader()
reader.SetFileName(filename)

mapper = vtk.vtkPolyDataMapper()
if vtk.VTK_MAJOR_VERSION <= 5:
    mapper.SetInput(reader.GetOutput())
else:
    mapper.SetInputConnection(reader.GetOutputPort())

# actor
actor1 = vtk.vtkActor()
actor1.SetMapper(mapper)

# outline
reader = vtk.vtkSTLReader()
reader.SetFileName(filename2)

mapper2 = vtk.vtkPolyDataMapper()
if vtk.VTK_MAJOR_VERSION <= 5:
    mapper2.SetInput(reader.GetOutput())
else:
    mapper2.SetInputConnection(reader.GetOutputPort())

actor2 = vtk.vtkActor()
actor2.SetMapper(mapper2)
actor2.GetProperty().SetOpacity(0.4)
actor2.GetProperty().SetColor(tomato)

#####

# create a rendering window and renderer
ren = vtk.vtkRenderer()
renWin = vtk.vtkRenderWindow()
renWin.SetSize(800,600)
renWin.AddRenderer(ren)

# create a renderwindowinteractor
iren = vtk.vtkRenderWindowInteractor()
iren.SetRenderWindow(renWin)

#ren.AddActor(actor1)
hippo1 = vtk.vtkOrientationMarkerWidget()
hippo1.SetOrientationMarker(actor1)
hippo1.SetViewport(0.4,0,1.0,0.6);
hippo1.SetInteractor(iren)
hippo1.EnabledOn()
hippo1.InteractiveOn()
ren.ResetCamera()
#ren.AddActor(actor2)
hippo2 = vtk.vtkOrientationMarkerWidget()
hippo2.SetOrientationMarker(actor2)
hippo2.SetViewport(0,0,0.6,0.6);
hippo2.SetInteractor(iren)
hippo2.EnabledOn()
hippo2.InteractiveOn()
```



```
ren.ResetCamera()

axesActor = vtk.vtkAxesActor()
axes = vtk.vtkOrientationMarkerWidget()
axes.SetOrientationMarker(axesActor)
axes.SetViewport(0.75,0.75,1.0,1.0);
axes.SetInteractor(iren)
axes.EnabledOn()
axes.InteractiveOn()
ren.ResetCamera()

# enable user interface interactor
iren.Initialize()
renWin.Render()
iren.Start()
```

Appendix D : Voxel Volume

```
import matplotlib.pyplot as plt
from mpl_toolkits.mplot3d import Axes3D
import numpy as np
import nibabel as nib

img = nib.load("6307_l_hippo.nii.gz")
data = img.get_data()
print(len(data))

#print data
print data.shape
#print data[0][1]

datalist=[]
for i in range(0,data.shape[0]):
    for j in range(0,data.shape[1]):
        for k in range(0,data.shape[2]):
            if data[i][j][k] == 1:
                datalist.append([i,j,k])

#print len(datalist)
N=len(datalist)
img_data = np.asarray(datalist)
print "Voxel count(L) =",N

img = nib.load("6307_r_hippo.nii.gz")
data = img.get_data()
print(len(data))

#print data
print data.shape
#print data[0][1]

datalist=[]
for i in range(0,data.shape[0]):
    for j in range(0,data.shape[1]):
        for k in range(0,data.shape[2]):
            if data[i][j][k] == 1:
                datalist.append([i,j,k])

#print len(datalist)
N=len(datalist)
img_data = np.asarray(datalist)
print "Voxel count =",N
```